Relation Between Weld Parameters And Weld Quality In AC Resistance Spot Welding Aluminium,

M.Sc. Thesis

Cierick Goos

June 1998

Examining board:

Prof.Dr. G. den Ouden	**(TU Delft, TMC-3)**
Prof.Dr.Ir. S. van der Zwaag	**(TU Delft, PT-2)**
Ir. T. Luijendijk	**(TU Delft, TMC-3)**
Ir. A.W.M. Bosman	**(Hoogovens R&D)**
Ir. O.J. Hana	**(Hoogovens R&D)**

Abstract

The two main areas of concern when resistance spot welding aluminium are the electrode lifetime and inconsistent weld quality. During welding the electrodes deteriorate, they erode and become rough. The weld quality is negatively affected by this deterioration. The welding electrodes have to be replaced before welds are produced with insufficient quality.

The objective of this research project was to determine the important features of the welding process and if these features could be linked to weld quality, to gain insight into the relation between welding parameters and weld quality. During welding a number of welding parameters can be measured such as welding current, welding voltage, electrode displacement or electrode force. Because of the importance of the dynamic resistance the electrical signals were selected as the parameters to be monitored. Welding current and welding voltage were selected, also because they are relatively easy to measure and it is clear which physical information they represent.

These electrical welding signals are distorted by the high magnetic field caused by the high welding current. A method was developed to clear the measured welding voltage signals of the inductive components. A specially for this project designed data analysis program was used to investigate the electrical welding signals. The signals from the first cycle of welding were found to be most important. The quality could be linked to features of the signals from the very first halfcycle of welding. This link between measured welding parameters and weld quality can be the basis for an on-line quality control system. Such a system could guarantee spot welds in welded products to be 100% error free without the need for destructive tests.

It was found that both the level as well as the form of the dynamic resistance curve for the electrode to sheet interface is unaffected by the deterioration of the welding electrodes. At the sheet to sheet interface the situation is reverse. The sheet surfaces are still the same (always fresh surfaces) but the dynamic resistance curve of this interface changes. An altering situation at the electrode-sheet contact (the electrode face becomes flat and rough) causes a change in dynamic resistance at the faying interface.

A model is proposed to explain the random occurrence of interface failure welds at the end of the electrode life. In this new model all welds beyond the electrode life are considered of low quality and not only those who fail as interface failure in a destructive test. Weld quality should thus not only be assessed on basis of a plug or an interface failure in tensile loading tests.

Index

1. Introduction

Resistance spot welding is still the method most widely used in joining sheet metal components for the automotive industry. Thousands of spot welds are used to assemble an automobile. The process is widely used because it has historically proven to be a reliable, cost-effective method of joining. New materials (such as aluminium alloys) are being used, to help reduce vehicle weight and improve corrosion resistance. These new materials are more difficult to resistance spot weld than the conventional, (un)coated, low carbon steels they are replacing.

A rapid, low cost, reliable joining or assembly process is required to make aluminium an acceptable material for construction. Although aluminium is more difficult to resistance spot-weld it remains one of the more attractive assembly joining methods. This is because it is simple in principle and it is a process currently in world-wide use by automobile manufactures.

Two areas of concern when resistance spot welding aluminium are the electrode lifetime and inconsistent weld quality. During welding the electrodes deteriorate, they erode and become rough. The weld quality is negatively affected by this deterioration. The welding electrodes have to be replaced before welds are produced with substandard quality.

The objective of this research project was to gain insight into the relation between welding parameters and weld quality. During welding a number of welding parameters can be measured, for this project the welding voltage and current signals were selected. A relation between welding parameters and weld quality can be the basis for an on-line quality monitoring system. So the spot welds in welded products can be guaranteed 100% error free without the need for destructive tests.

The experimental work for this project was carried out at the joining technology group of Hoogovens Research & Development in co-operation with Delft University of Technology group of Welding Technology & Non-Destructive Testing. The project was incorporated in the Hoogovens Car=Lite programme which aims on reducing the weight of monocoque autocar bodies.

2. Theoretical background

2.1. Description of the welding process

A spot weld is produced between two sheets of material in contact by applying a force to the sheets and passing a high electrical current through them for a short period of time. The widely used and relatively simple single phase AC resistance spot welding machine is basically a large transformer as shown in figure 2.1. Copper (or copper alloy) welding electrodes are used to apply the force and current to the sheets. These electrodes are internally water cooled.

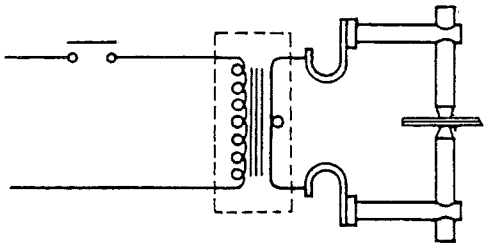

Figure 2.1: Typical single phase spot welding circuit [1].

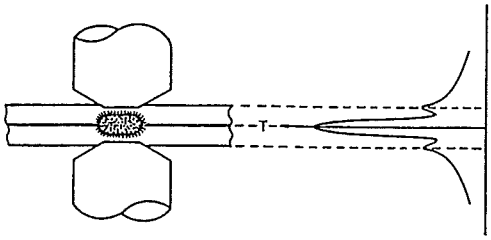

Figure 2.2: heat generation during spot Welding [2].

Resistance heating effects cause the metal to melt and form a molten nugget, figure 2.2. Upon weld termination, the molten nugget cools down and solidifies into a fused, welded joint [3]. Figure 2.3 gives a schematic representation of a weld schedule. First the parts are firmly pressed together in the squeeze period. Then in the welding period a high current is passed through the sheets and a molten nugget is formed. When the current is shut off the holding period starts and the nugget solidifies, thereafter the pressure is released to complete the cycle.

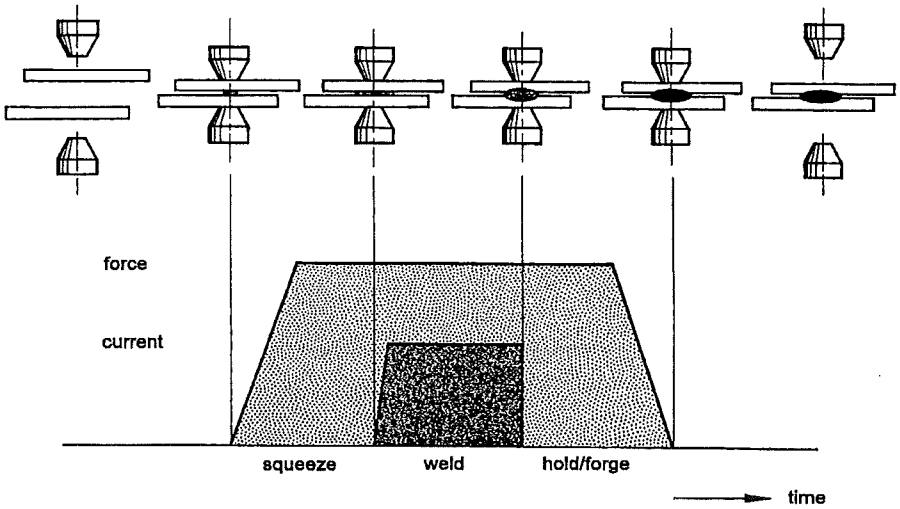

Figure 2.3: Schematic representation of a weld schedule [4].

The welding current can be affected in two different ways: by changing the transformation ratio of the transformer by a stepped switch; or by electronic governing of the ignition point in the electronic contactor. Electronic governing (heat control) changes the shape of the current waveform. At maximum heat input the waveform is sinusoidal, as shown in figure 2.4, while at reduced heat input there is an interval between the individual halfwaves, as shown in figure 2.5.

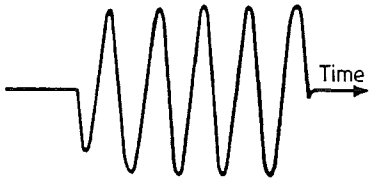

Figure 2.4. Current waveform at maximum heat input [5].

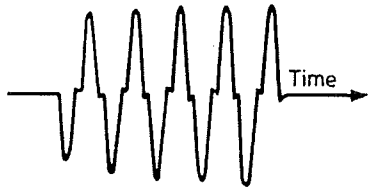

Figure 2.5. Current waveform at reduced heat input [5].

The conduction time is the period in which current flows through the electrodes. Tests performed by Spinella and Patrick [6, 7] indicate that the weld nugget quality and electrode life performance substantially improves with increasing conduction time. Proper sizing of alternating current (AC) resistance welding transformers can significantly extend electrode life performance.

Resistance spot welding behaviour of aluminium is entirely different to that of steel. For steel spot welding the high bulk resistivity is an important controlling factor, whereas for aluminium the surface characteristics are far more important. Aluminium alloys have 2.5 to 3.5 times the electrical and thermal conductivity of steel and less than half the melting temperature. A threefold increase in welding current over that of steel at about one fourth to one third of the welding time is required to achieve equivalent nugget sizes. In addition, the resultant nugget size is greatly influenced by the magnitude of the interface resistances. If these interface resistances are low, then for the same welding current less heat is generated, this can result in a smaller nugget [9].

2.2. Dynamic resistance

The resistance of the sheets between the electrodes is not constant throughout the welding cycle but is dynamic in nature. An important difference between aluminium and steel welding behaviour can best be illustrated by comparing the dynamic resistance curves shown in figure 2.6. Aluminium starts at a high initial resistance of greater than 150 μΩ and quickly drops to about 25 μΩ as the molten nugget is formed in the first halfcycle of welding. Thereafter, the resistance continues to decrease slightly with each halfcycle. Although the resistivity of molten aluminium is 9 to 10 times that of aluminium at room temperature, the resistance continues to decrease because of the increasing cross sectional area of the molten nugget. If sufficient current is not available to form a molten nugget during the first halfcycle, additional welding time will not produce nugget growth. For (un)coated steel after the initial drop in contact resistance, the resistance continues to rise as the resistivity of the solid steel increases with increasing

temperature until the molten nugget begins to form at a much higher temperature than is the case with aluminium. The resistance for steel then decreases with increased weld time as the nugget begins to grow [8].

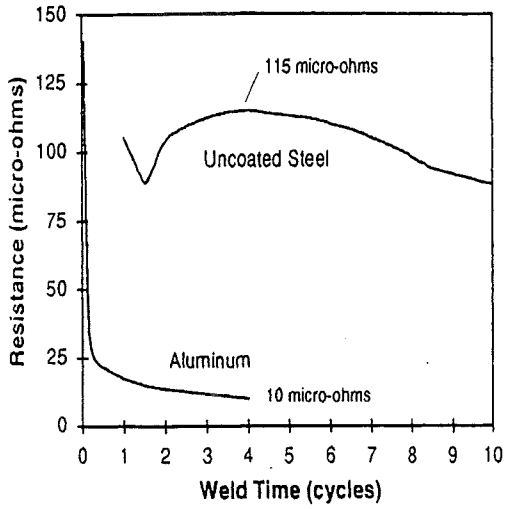

Figure 2.6: Dynamic resistance curves of aluminium and steel [8].

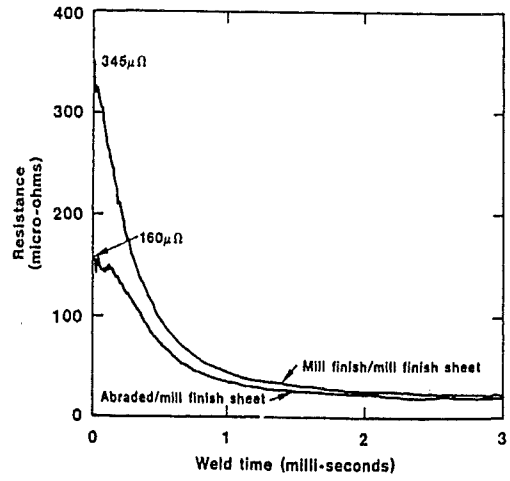

Figure 2.7: Dynamic resistance during first ¼ cycle of welding [9].

For aluminium the dynamic resistance curves are mainly determined by the dynamic characteristics of the contact resistances, the resistances of the sheet-sheet and electrode-sheet contacts. Contact resistance and thus dynamic resistance curves also depend on the surface condition of the sheet as can be seen in figure 2.7. Contact resistances play a major role at the very beginning of the weld cycle, because 80% of the nugget growth occurs during the first cycle of welding [9].

2.3. Electrode deterioration mechanism

2.3.1. Mechanical contacts

No solid body has a perfectly plane surface, and if contact members were infinitely hard, no load could bring them to touch each other in more than three points [10]. But since actual materials are deformable, these points become enlarged to small areas and simultaneously new contact points may set in. The sum of all these areas or spots is the load bearing area, in which the contact pressure is finite. The load bearing area can be generated merely by elastic deformation. However, because of their unevenness, the contact members, even though they may be nominally flat, mostly touch each other in areas that are more or less plastically generated.

The load bearing area usually is much smaller than was supposed about seventy years ago. If, for example, nominally plane bodies were placed on top of each other the whole covered area

was often called the contact surface. It is more correct to call this the apparent contact area. The load bearing area may be an order of magnitude smaller than the apparent contact area [10].

With increasing radius of curvature of two contact members the elastic contact area for a certain load increases, and, theoretically, would finally elastically produce arbitrarily large contact areas. Actually, a limit is reached because of the unevenness of the contact faces. When a contact is made the asperities are hit first, and they may deform plastically and strain harden, while the underlying metal may deform mainly elastically [10].

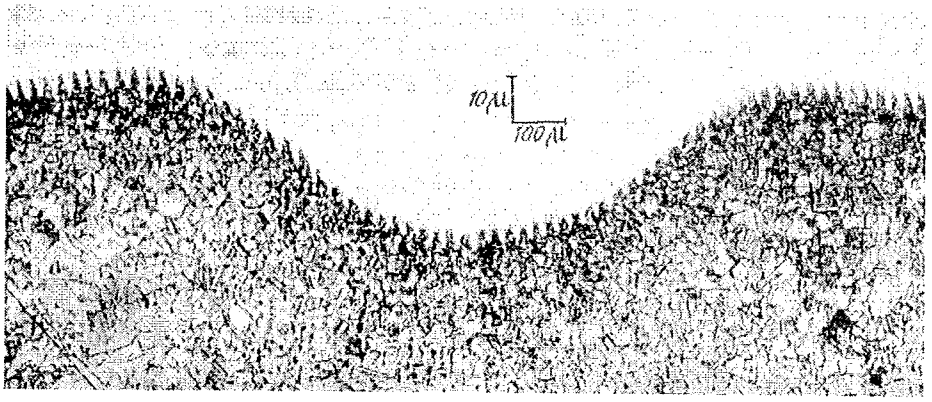

Figure 2.8: Deep indentation in annealed grooved copper, showing the persistence of the grooves in the indentation [10].

The remarkable persistence of asperities during bulk deformation is shown in figure 2.8. The material, copper, was initially annealed. The fact that nevertheless the asperities were not obliterated is understandable if one considers that the asperities yield plastically with about the same percentage of their height as the underlying plastically deforming material does with respect to its thickness, which is much greater than the height of the asperities [10].

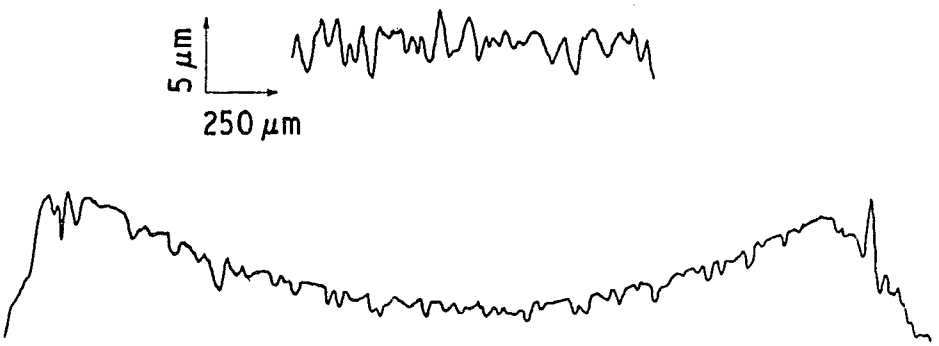

Figure 2.9: Profile of brinell impression in a gold block (most of the curvature of the indentation has been cut out). The upper profile shows part of the undeformed surface [11].

Another example, figure 2.9 shows a surface profile across a Brinell hardness indentation. The apparent contact area, used to assess the hardness, is divided into a multitude of microcontacts. It is doubtful whether there is any experimental evidence that the real area of contact is proportional to the load, but rather good experimental evidence that the apparent area is proportional to the load [11]. Contacts between nominally flat surfaces are known to occur as a number of clusters of microcontacts, the position of these clusters being determined by the large scale waviness of the surface, and the position of the microcontacts by the small scale surface roughness [11].

2.3.2. Electrical contacts

Regarded from the aspect of current conduction the load bearing area may consist of three different types of areas (in order of decreasing conductivity):

- portions with metallic contact; through these areas the current passes without perceptible transition resistance in the interface, just as it does between different crystallites in a compact metal;
- quasi-metallic spots; these are film covered areas on which the films are sufficiently thin to be easily permeable by the electron current by means of the tunnel effect irrespective of the proper resistivity of the film material. Typical films of this kind are the thin layers of physical or chemical bonded oxygen atoms which, in air, are formed on any clean metal surface;
- areas covered by thicker multi-molecular alien films, particularly visible tarnish films, such areas are practically insulating.

For resistance spot welding the contact area can be simplified by dividing it in only two types, good conducting areas with metallic contact and non conducting areas (figure 2.10). It will be convenient to have a short name for the conducting contact areas, and in the following they are called a-spots, a widely accepted term [10].

The expression contact resistance is often used. This term was coined at a time when it was believed that the metallic contact surface itself accounted for this observed transition resistance. One may theoretically expect that the discontinuity of the crystal lattice order in perfectly clean contacts will reflect electrons and produce a transition resistance. However, such resistances are extremely small and have not been observed in contacts. Actually, what is measured as contact resistance is the consequence of current flow being constricted through small conducting spots, as shown in figure 2.11. The contact resistance always is or implies a constriction resistance [10].

Summing up, it can be seen that not only the load bearing contact area is very small, but also that only a fraction of it may be electrically conducting. In any case, the current flow lines are bent together through narrow areas, causing an increase of resistance compared with the case of a fully conducting, apparent contact surface [10].

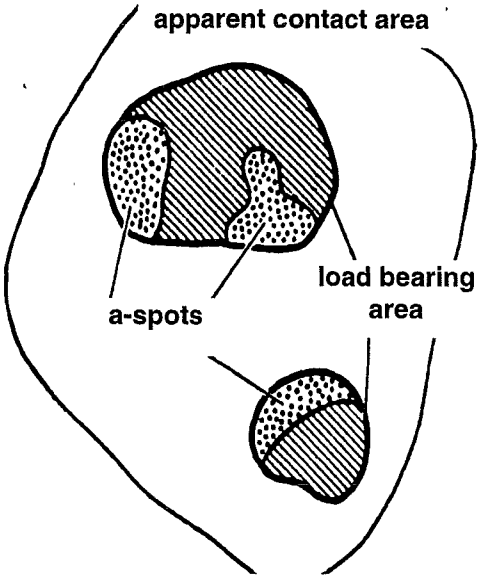

Figure 2.10: Apparent contact surface, loadbearing contact area containing insulating spots (shaded) and conducting a-spots (dotted) [10].

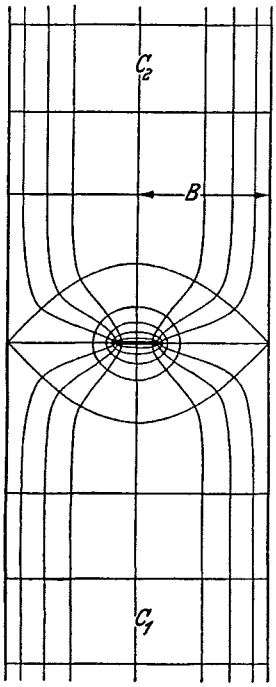

Figure 2.11: Lines of current flow and equipotential surfaces of a current constriction [10].

The constriction resistance will be partly determined by the number and size of the microcontacts (a-spots) and partly by their grouping into clusters. The contact resistance is no single valued function of the total electrical contact area, because its subdivided into small a-spots of which the number, size and grouping into clusters is unknown. This is the reason why the total conducting contact area can not be inferred with reasonable accuracy simply from a resistance measurement [10]. It is impossible to deduce anything about the real area of contact directly from measurements of the constriction resistance, except an upper limit; and the actual value can be a small fraction of this [11].

Whenever there is a reasonably large number of not too small contacts the constriction resistance is close to that observed if the entire area of the cluster were in electrical contact. If an insulating film covers the mechanical area of contact, so that electrical contact occurs by a large number of small cracks in the film, the resistance may be almost as low as with no film [11].

When current is applied to a contact, it is heated by the current flowing through it. If the contact is symmetrical and both contact members are of the same material the highest temperature is localised in the contact surface. For such contacts an indirect method exist, to determine the contact temperature from the contact voltage. This relationship uses the fact that the heat is flowing along the same paths as the current. Because of the symmetry there is no reason for heat transfer from one member to the other. The results of this relation are shown for copper in table 1, note the rapid increase in contact temperature with contact voltage [10].

Table 1: Relation between potential drop across the contact and contact temperature [10].

		Softening		melting
V (V)	0,03	0,12	0,3	0,43
T (°C)	16	190	700	1065

During welding the current constricting a-spots are rapidly heated up, this causes the spots to widen. At the beginning of welding the current conducting area grows very rapidly, this also implies a fast decrease in the constriction resistance.

In the spot welding machine the welding electrodes contact the two overlapping sheets on the outside surfaces and local plastic deformation of the bulk material occurs and also at the contact surfaces of both sheets. In addition, there is also the chance of sliding between the two surfaces in contact. This shows why metallic contact and therefore electrical conduction can be easily realised through heavy contaminant layers [12].

2.3.3. Electrode deterioration

The electrical constrictions on the electrode to sheet interface coupled with the welding current are primarily responsible for electrode deterioration. Before the electrode contacts the aluminium sheet, there is a layer of oxide on the sheet. When the electrode comes in contact with the asperities of the sheet, it causes oxide fracture, allowing only small areas for current conduction (figure 2.12), as explained in more detail in sections 2.3.1 and 2.3.2. During welding some surface melting occurs as can be seen with optical magnification of the indented surfaces after welding [13].

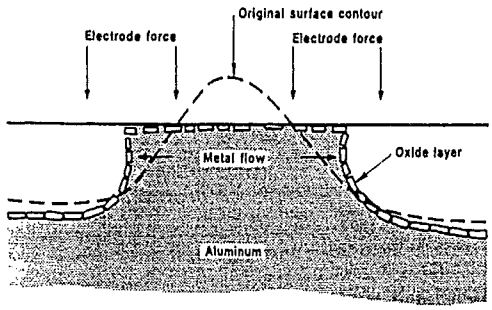

Figure 2.12: Making electrical contact [9].

The molten aluminium in contact with the electrode starts a catastrophic process. Aluminium sticks to the electrodes and diffuses into the high conductivity copper (and thereby decreasing the conductivity) causing additional local resistance heating of the electrode surface. In addition, the copper-aluminium intermetallics formed are brittle and subsequent mechanical contact and diffusion bonding to the sheet causes fracture of the electrode face, leaving a pitted electrode. The now rough electrode tip creates high local concentrations of current flow which cause even more severe hot spots, more molten aluminium, more diffusion, and faster electrode deterioration [3].

On new electrodes there is a repeated action of "pickup" from the aluminium surface and an erosive "pullout" of copper from the face of the electrodes. After 50-100 welds the whole contact area of the electrodes is coated with aluminium. Hereafter the erosive process predominates and there will be a steady loss of copper from the face of the electrodes [14, 5]. This electrode deterioration process proposed by Patrick et al. [9] is graphically depicted in figure 2.13.

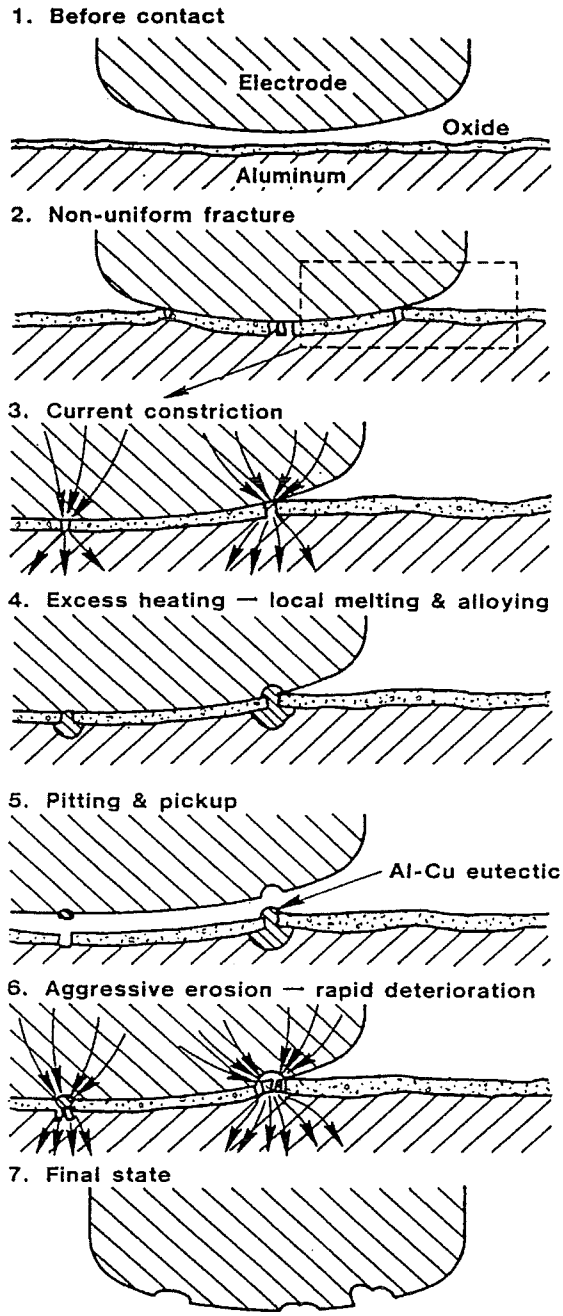

Figure 2.13: Electrode deterioration mechanism [9].

3. Experimental procedure

3.1. Experimental background

As stated earlier 80% of the nugget growth occurs during the first cycle of welding [9]. In this first cycle of welding the dynamic resistance of the aluminium decreases more than a decade in value. The dynamic resistance falls a decade in value in less than 5 ms (less than ¼ cycle). This is caused by the rapid growth of the conducting a-spots. Thus the first cycle of welding is very important in resistance spot welding.

A monitoring system therefore should gather a lot of information especially during the first cycle of welding. The entire waveform of a welding parameters should be measured and not just the average value for the whole welding period. All this data should be processed to extract the important features. Furthermore, the amount of data must be reduced without losing the important information.

In this research project the objective was to find which are important features of the welding process and whether these features could be linked to weld quality. During welding a number of welding parameters can be measured such as welding current, welding voltage, electrode displacement or electrode force. Mechanical parameters such as electrode displacement or electrode force are strongly influenced by the welding machine itself (stiffness of the frame for instance). These mechanical parameters can therefore never be machine independent. Because of the importance of the dynamic resistance the electrical signals were selected as the parameters to be measured. Welding current and welding voltage were selected, also because they are relatively easy to measure and its clear which physical information they represent.

To link weld quality to features of the welding voltage and current signals, data of high and low quality welds was needed. New electrodes normally produce "good" welds. When the electrodes are worn they produce welds of lower quality. To get "good" and "bad" weld data with the same welding electrodes, electrode life tests were done. During these tests data was gathered for each individual weld. The tests were stopped when the electrodes were producing low quality welds, beyond the standard life of the welding electrodes. With the same electrodes welds of good quality (at the strart of the test) and of substandard quality (at the end of the test) were made.

3.2. Experimental set-up

For all welding experiments a single phase alternating current (AC) pedestal type resistance welding machine (315 kVA, 50 Hz) was used. The weld schedule consisted of the following stages:

squeeze time:	20 cycles (0.4 s)
weld time:	4 cycles (0.08 s)
hold time	8 cycles (0.16 s)

The electrode force was set at 1.8 kN, the electrodes used are shown in figure 3.1 and are made of a class 2 CuCr1Zr alloy (standardised classification, ISO 5182). The face of these electrodes is rounded (R=40 mm).

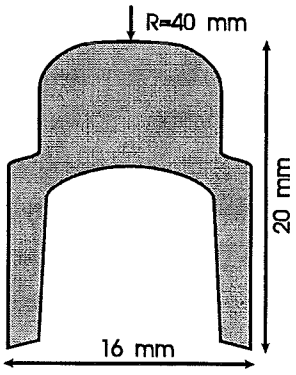

Figure 3.1: Cross-section of a welding electrode

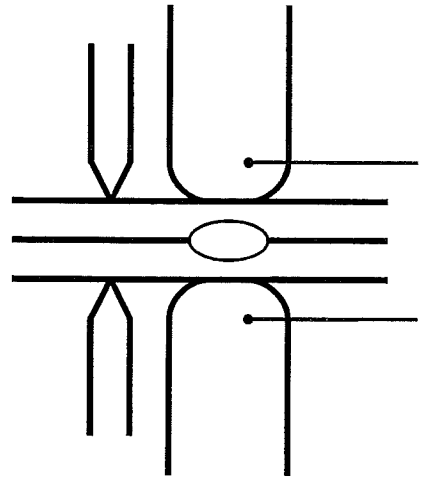

Figure 3.2a: Experimental arrangement for measuring electrode voltage and sheet surface voltage.

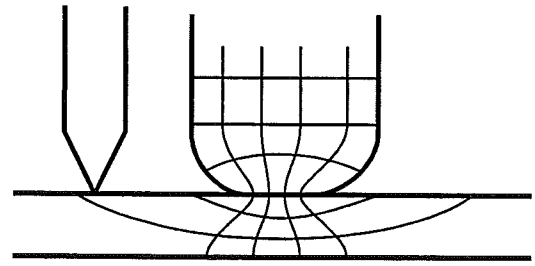

Figure 3.2b: Current flow and equipotential lines in a welding situation.

The experiments were carried out using pickled AA 5754 aluminium sheet of 1.2 mm thickness. During welding the welding current and welding voltage were measured and stored using a Nicolet 420 digital storage oscilloscope. The welding voltage was measured on the welding electrodes and on the sheet surface. Electrical pick-up leads were brazed onto the electrodes. These pick-up leads were attached close to the electrode face, for the measurement of the electrode voltage. The sheet surface voltage was measured with small spring mounted electrodes located along side the welding electrodes (figure 3.2a). The potential that is measured with the sheet

surface electrodes, is that of the material somewhere between electrode-sheet and sheet-sheet interface (figure 3.2b).

The stored current and voltage waveforms were analysed off-line with a data analysis program. The program code was developed by the author specially for this research project. The data analysis program can extract a number of parameters from the stored current and voltage waveforms such as the conduction time, RMS. voltage and RMS. current. For more details about the data analysis program see appendix A1.

The weld tests were carried out according to the French AFNOR standard A87-001 (December 1994). Most welds were made on 50 mm wide strips, the welds were placed 30 mm apart (45 welds per strip). The welding speed was set at 30 welds per minute, this is as close as possible to the welding speed in production schedules.

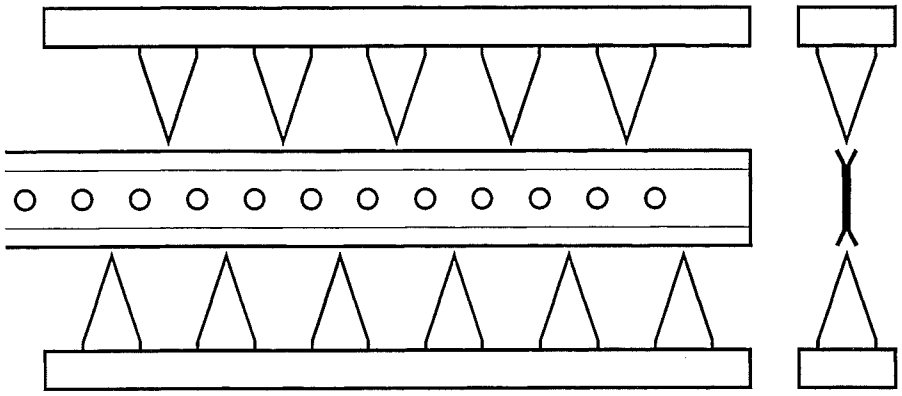

Figure 3.3: Schematic representation of the tool used for destructively testing the welded strips.

The strips were destructively tested with the tool shown in figure 3.3, the spikes of this tool force the sheets apart and cause the welds to fail. Welds can fail in two different ways, figure 3.4. The weld can tear a plug from the sheet, this is considered a good weld. Fracture can also occur through the weld itself, this is called an interface failure and is considered a bad weld. The strips are tested and judged on the appearance of the failed welds, plug or interface failure, good or bad. Another destructive test is the cross tension test shown in figure 3.5. In this test the specimen is tested in a tensile testing machine and the maximum load (cross tension strength) of the weld is measured. If there is a plug pulled from the sheet the diameter of it is also measured.

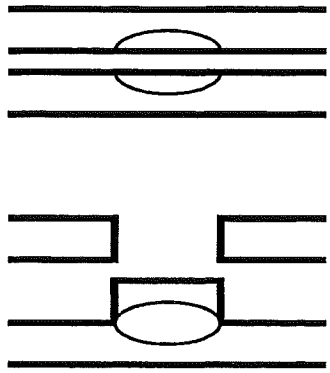

Figure 3.4: Two types of weld failure: interface failure (above) and plug failure (beneath).

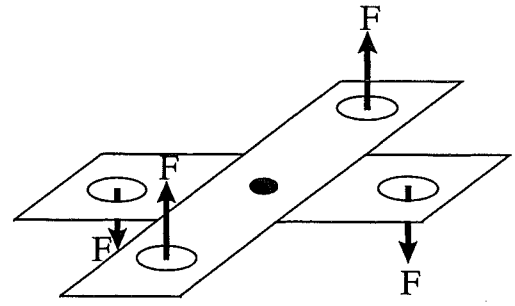

Figure 3.5: Cross tension test.

3.3. The compensation coil

The high alternating current creates a weld but also causes a high magnetic field. When electrical measurements are carried out during welding this magnetic field can cause distortion of the electrical signals. The electrode to sheet contact and the sheet to sheet contact are metallic contacts with a real resistance. Therefore the voltage signal over a weld should be in phase with the current signal Therefore the real voltage signal looks like figure 3.6a. The electromagnetic flux that is transmitted by the welding machine is picked up by the measurement circuit and causes an additional voltage signal. This inductive signal is depicted in figure 3.6b, this signal is in phase with dI/dt, it has a phaseshift of 90° prior to the current and real voltage signals. The sum of these two signals is the measured signal, shown in figure 3.6c, the signal is out of phase with the welding current. The amount of phaseshift is determined by the amplitude of the inductive signal relative to the amplitude of the real signal.

The inductive component in the measured signal can be compensated for by placing a compensation coil in the throat of the welding machine. The coil is placed close to the welding electrodes. The signal from such a coil is depicted in figure 3.6d, this is a true inductive signal and is thus proportional to the inductive component in the measured signal. By adjusting the amplitude the coil signal can be scaled to exactly the same form as the inductive component in the measured signal (figure 3.6e). It is identical to the inductive component in figure 3.6b. Subtracting the scaled coil signal from the measured voltage signal leads to the compensated signal in figure 3.6f, which is the same as the original real signal in figure 3.6a.

The idea to use a coil to compensate for the magnetic field during welding was published by W.L. Roberts [15] back in 1951. He connected a compensation coil in series with one of the voltage pick-up leads, thereby subtracting the coil signal from the measured signal. The scaling of the coil signal was done by adjusting the orientation and position of the compensation coil. By adjusting the coil in this way the inductive coupling between the welding circuit and the coil is changed and thereby the amplitude of the coil signal can be manipulated.

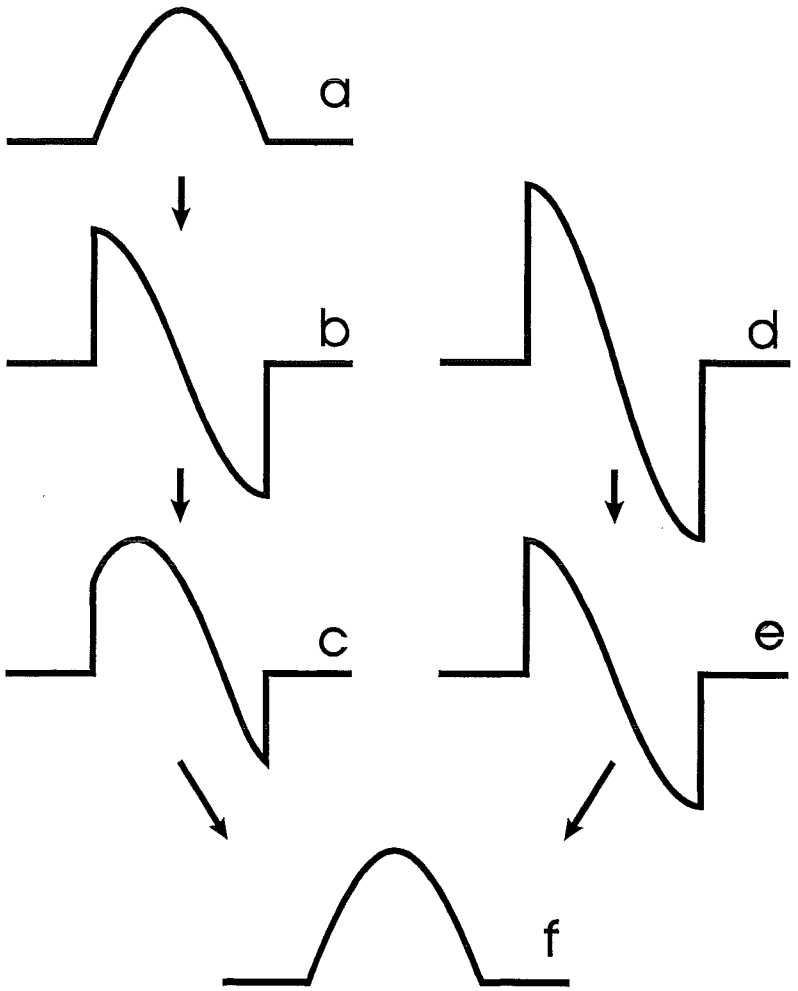

Figure 3.6: Distortion of voltage signals and the compensation therefore;
a) real signal, b) inductive component, c) measured signal,
d) compensation coil signal, e) scaled coil signal and
f) compensated signal.

In this project a somewhat different approach was chosen. A simple coil (insulating wire and tape) was attached to the bottom electrode holder. The coil was placed as close as possible to the electrode. The electrical signal of this coil was measured and stored simultaneously with the other signals. The stored signal was then used to compensate off-line. The scaling of the coil signal and subtracting it from the measured voltage signals was done numerically after welding. The algorithms needed for this off-line compensation were developed by the author and incorporated in the data analysis program code. The advantage of this approach is that the coil is now in a fixed position and the compensation is done separately for each weld.

The sheet surface and electrode voltage as well as the current waveforms are shown in figures 3.7 and 3.8, uncompensated and compensated for the magnetic field. In these figures as well as in the tables 2 and 3 it can be seen that the inductive term severely distorts the signals, it even dominates the curve for the sheet surface.

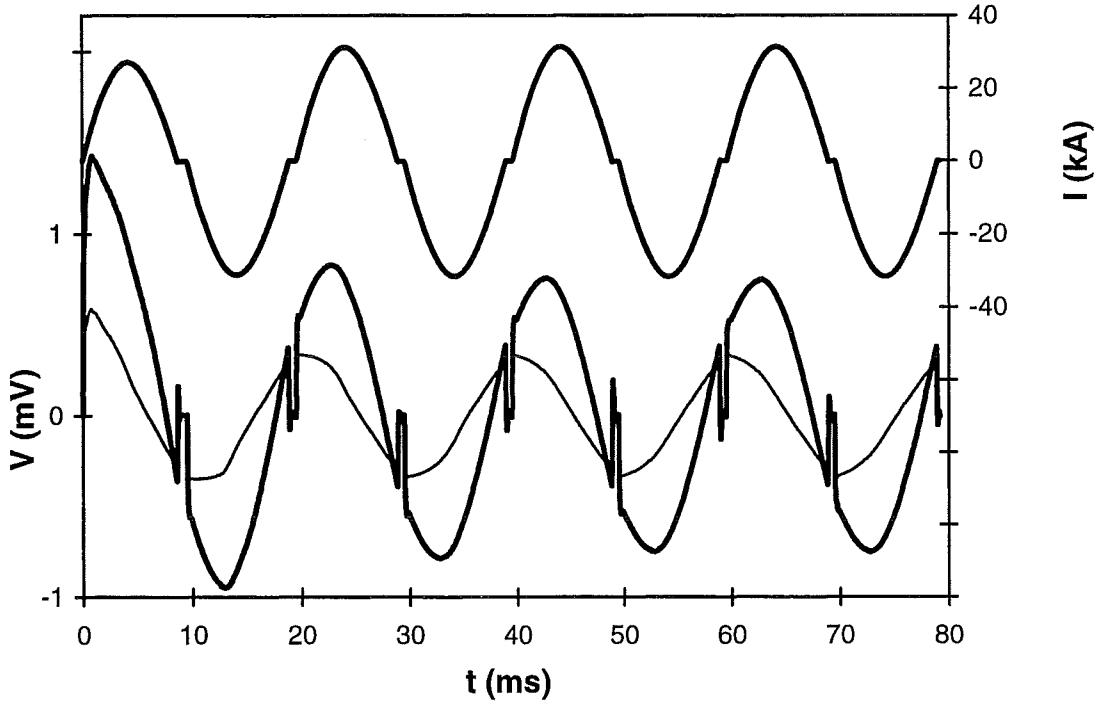

Figuren 3.7: Current (above) and uncompensated voltage signals of electrode (thick line) and sheet surface (thin line).

Table 2: Main output of data analysis program, without compensation (S1, weld 500)

half cycle	t_{aan} (ms)	I_{RMS} (kA)	$V_{sh\text{-}rms}$ (V)	$V_{el\text{-}rms}$ (V)	Q_{sh} (J)	Q_{el} (J)	A_{sh} (VA)	A_{el} (VA)
1	8.7	17.8	313	857	33	126	15940	29217
2	9.4	21.4	240	644	27	125	14279	19072
3	9.3	21.3	227	580	23	110	14247	18816
4	9.4	21.6	222	550	20	104	14286	18972
5	9.4	21.4	215	532	18	99	14020	18799
6	9.4	21.7	212	525	18	99	13974	18748
7	9.4	21.4	211	524	17	97	13963	18702
8	9.4	21.7	211	526	16	99	13985	18642

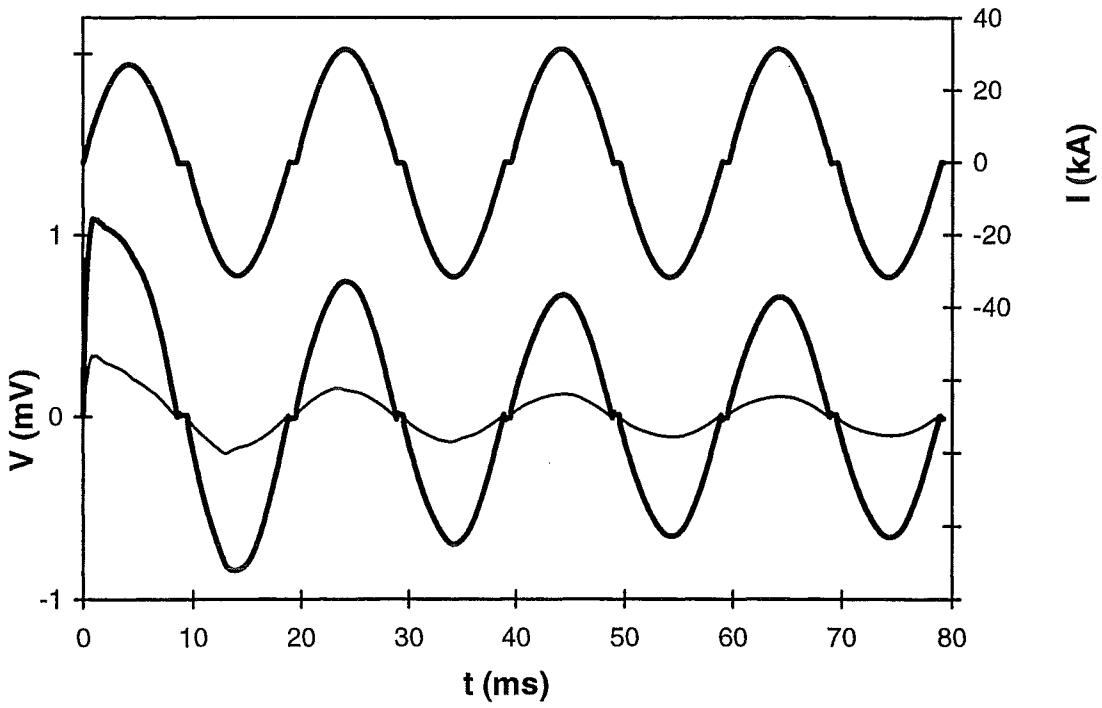

Figure 3.8: Same as 3.7 but with compensation of the inductive components in the voltage signals.

Table 3: Same as table 2 but with compensation of the inductive components in the voltage signals.

half cycle	t_{aan} (ms)	I_{RMS} (kA)	$V_{sh\text{-}rms}$ (V)	$V_{el\text{-}rms}$ (V)	Q_{sh} (J)	Q_{el} (J)	A_{sh} (VA)	A_{el} (VA)
1	8.7	17.8	204	760	33	126	4646	14335
2	9.4	21.4	128	584	27	125	735	1225
3	9.3	21.3	105	514	22	110	401	571
4	9.4	21.6	93	481	20	104	379	646
5	9.4	21.4	85	460	18	99	106	463
6	9.4	21.7	80	453	17	99	42	388
7	9.4	21.4	77	452	16	97	64	387
8	9.4	21.7	74	455	16	99	89	332

4. Results

4.1. Growth curve

In this research programme two different weld button sizes were used. A button with a diameter of 5.5 mm and a larger one of 7.0 mm in diameter. The smaller diameter of 5.5 mm is based on the rule that the diameter of the weld should be five times the root of the sheet thickness, this rule is often used when spot welding steel sheet. The larger weld button diameter of 7.0 mm was used because this was the diameter used in earlier research [16]. For each weld parameter setting three test runs were conducted (S1, S2, S3 with diameters of 5.5 mm and L1, L2, L3 with the larger diameter of 7.0 mm)

To determine the appropriate welding settings for these button sizes a growth curve was determined. In a growth curve the weld button size is plotted against the welding current (for a given welding schedule). The growth curve for the used material and welding schedule is shown in figure 4.1. For welding buttons with a 5.5 mm diameter an average current of 21 kA is needed and for 7.0 mm welds a welding current of about 25 kA is needed.

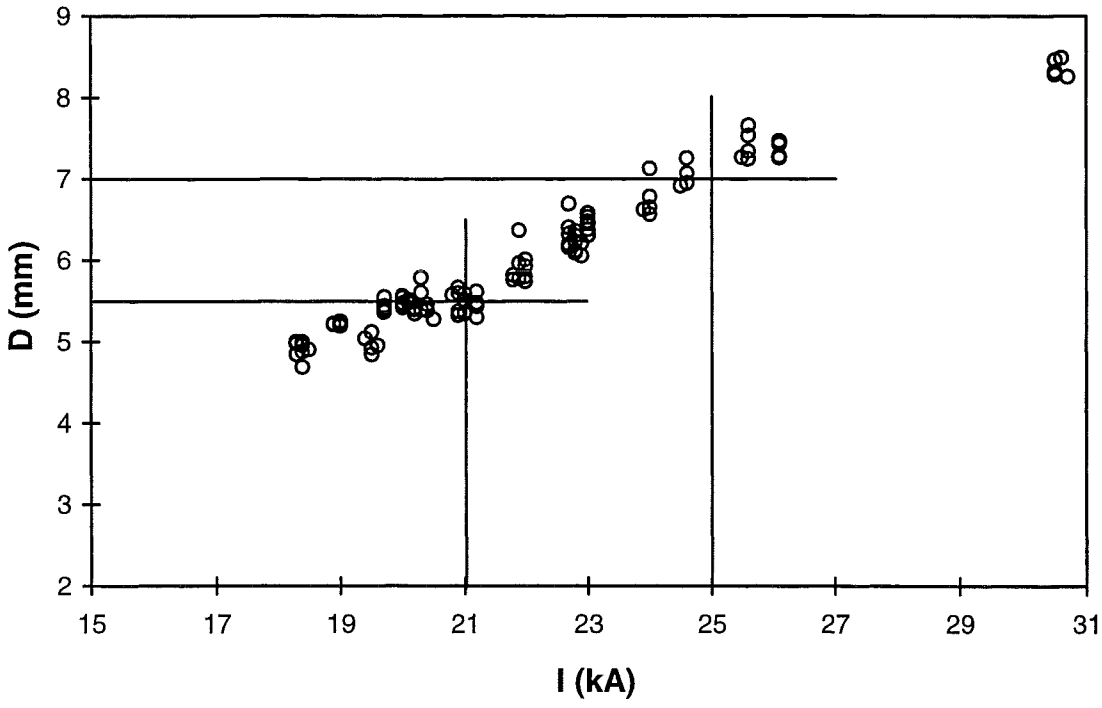

Figure 4.1: Growth curve, weld button diameter vs. welding current.

The welding tests for the growth curve were made on cross tension samples. Not only the diameter of the plug but also its cross tension strength was measured. In figure 4.2 it can be seen that this strength is proportional to the diameter of the plug. When a plug is pulled out of a sheet, the area over which the material is sheered off is proportional to the thickness of the sheet and the circumference of the plug. For a round plug the circumference is proportional to its diameter and then so is its cross tension strength.

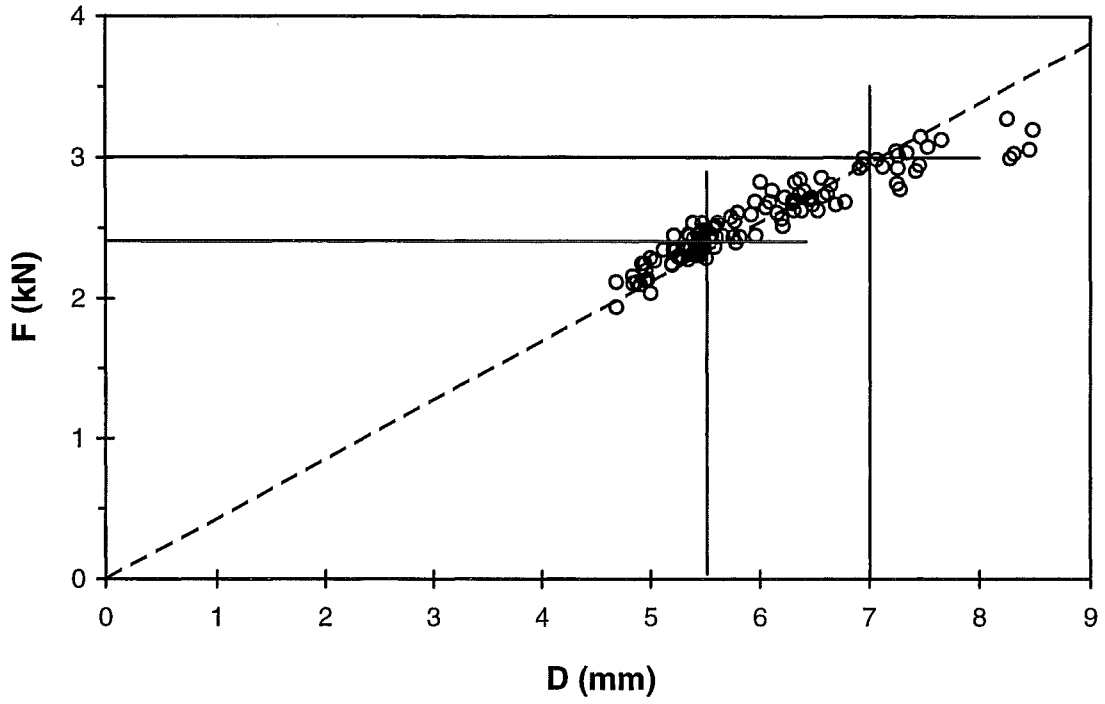

Figure 4.2: Weld cross tension strength vs. weld button diameter.

A high heat control setting was used for the welding trials. A welding current of 21 kA was achieved with the transformer set on tap 23 (out of 27) and the heat control on 775 (out of 1000), for the welding current of 25 kA the transformer was set on tap 24 and the heat control on 800. For more information about the welding current and machine characteristics see appendix A2.

4.2. The first test

For the first welding test (S1) the welding machine was set for weld buttons with a diameter of 5.5 mm. The test was ended when a total number of 4500 welds was made. The welding current (I_{RMS}) deviated very little over the welding trial, the welding current was fairly constant for each weld. For these experiments the welding machine can be considered a constant current source.

For this welding trial the welding voltage (V_{RMS}) and the welding energy (Q) both of the first half cycle of welding are plotted in the figures 4.3 and 4.4, both parameters were measured on the electrodes as well as on the sheet surface. These curves all show the same trend. For the first 1250 welds (region I) the signal is constant then it drops over the following 1000 welds (region II) thereafter it again has a more or less constant value (region III).

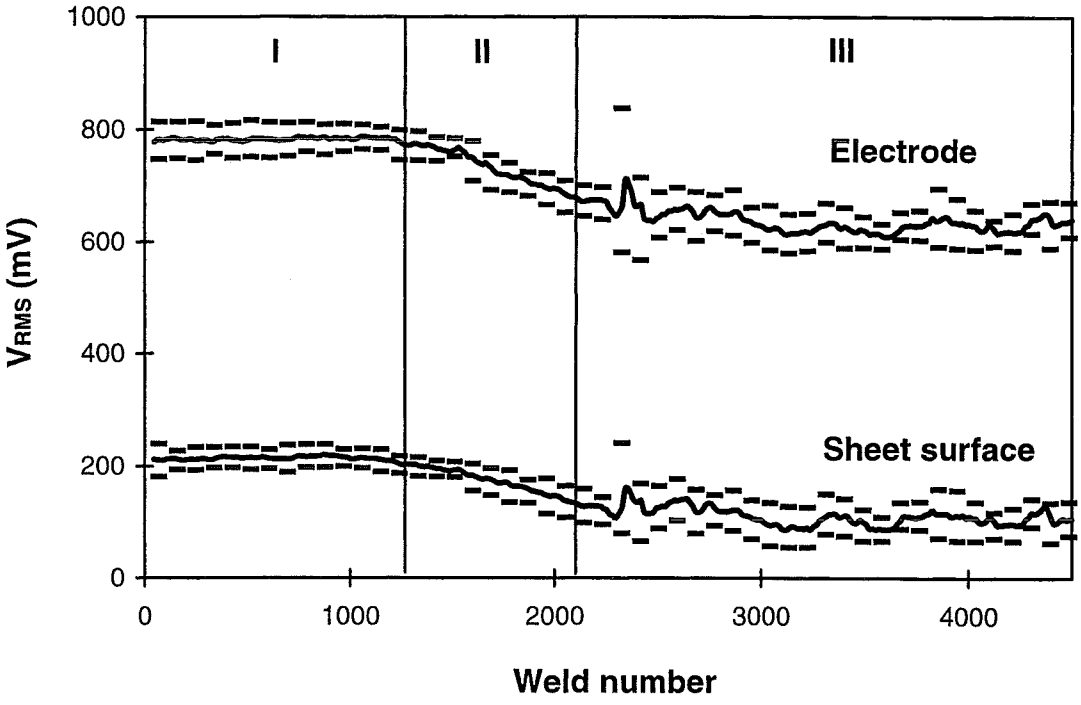

Figure 4.3: Moving average and scatter of the RMS. Voltage for the first half cycle of welding vs. the number of welds made (S1).

The same charts (V_{RMS} and Q vs. weld number) for the second half cycle show more or less the same trend but far less pronounced. On the charts for the third till eight half cycle the trend can not be seen, the values of the signals in these charts are fairly constant during the whole test. The first half cycle of welding contains the most information. It is the most important half cycle when monitoring the welding process. This was expected because of the sharp decrease in dynamic resistance when spot welding aluminium, within the first half cycle the resistance decreases almost to a constant value.

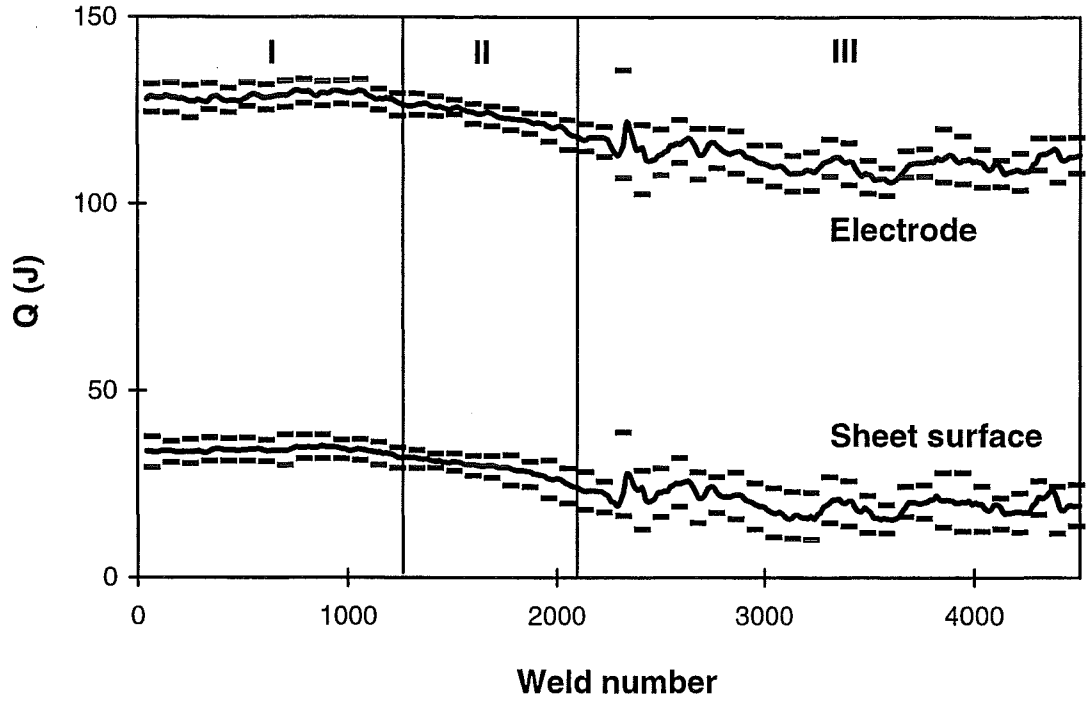

Figure 4.4: Moving average and scatter of the welding energy for the first half cycle of welding vs. the number of welds made (S1).

In figures 4.5 and 4.6 the voltage-current curves for the first cycle of welding are shown for a typical region I weld and a typical region III. In a voltage-current diagram a constant resistance gives a straight-line through the origin of the diagram, a higher resistance gives a steeper line. The high initial resistance causes a steep start of the VI-curve, the fall in dynamic resistance causes the curve to bend. In these experiments the weld formation always starts in the first quadrant of a VI-diagram, welding voltage and current are both positive. The second half cycle then is in the third quadrant where voltage and current are both negative. The welding signal starts in the origin of a VI-diagram then make a loop (clockwise) in the first quadrant and return in the origin; the loop is caused by the decrease in dynamic resistance.

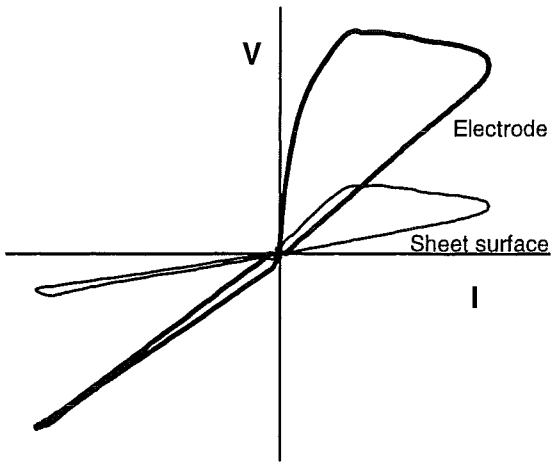

Figure 4.5: VI-Curves of the first cycle of welding for a typical region-I weld (S1, weld 500).

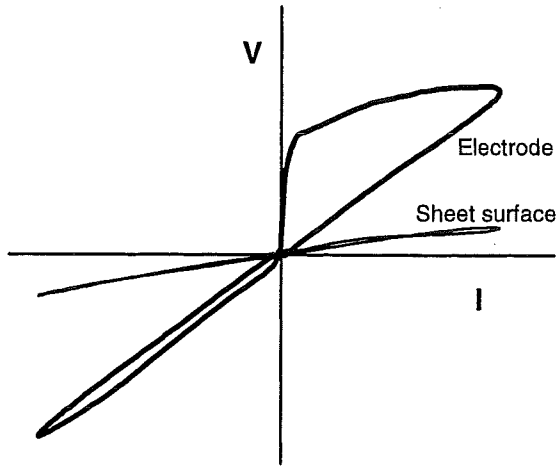

Figure 4.6: VI-Curves of the first cycle of welding for a typical region-III weld (S1, weld 3000).

In the figures 4.5 and 4.6 it can be seen that the VI-loop for the first half cycle of welding (first quadrant) is larger for the region-I weld, the region-III weld has a smaller loop. The area of this loop (A) can be calculated by integrating VdI over the first half cycle of welding. The values of this loop area (A-values) are plotted in figure 4.7. The curves show the same trend as the

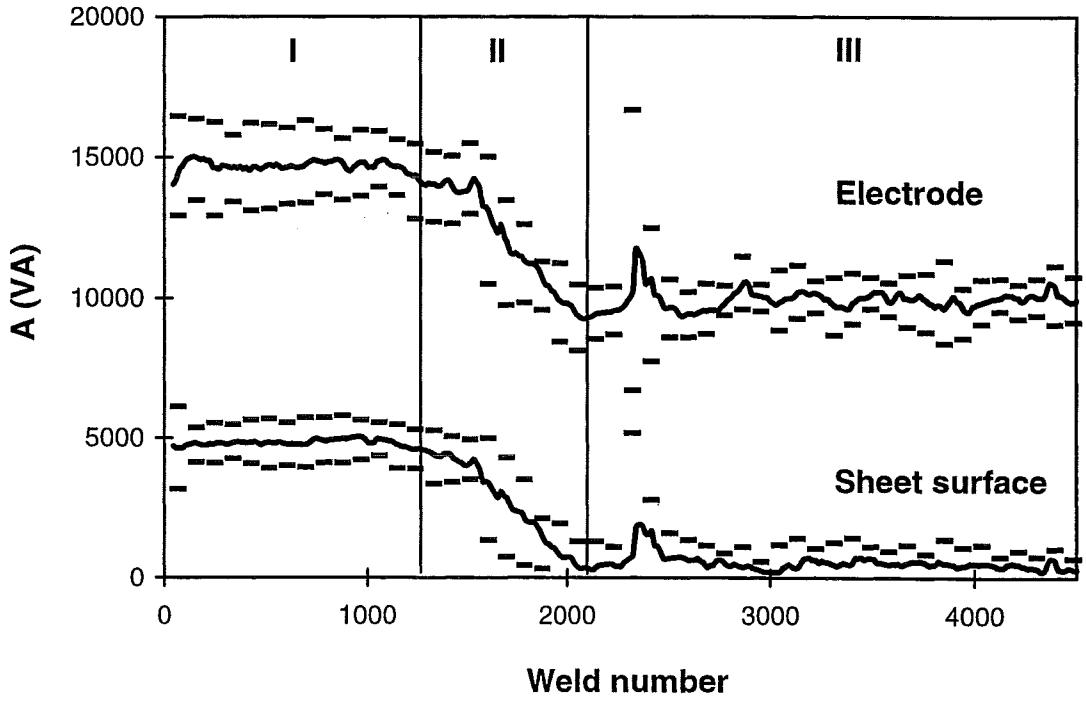

Figure 4.7: Moving average and scatter of the loop area for the first half cycle of welding vs. the number of welds made (S1).

voltage and energy curves but the trend is more pronounced in the loop area. The welding voltage and energy actually are functions of this loop form, this is why all these curves show the same trend (more or less pronounced). The actual value of the loop area (A) measured on the sheet surface reaches a value (in region III) of approximately zero, the sheet surface loop then becomes a straight line (figure 4.6).

After welding the welds were destructively tested and examined for the presence of interface failures. In figure 4.8 the individual values of the loop area (A) for the interface failures and the trendline for all welds are plotted. As can be seen in this figure the interface failures mostly occur in the lower region of the scatter band, most interface failures have an A-value beneath the trendline. But interface failures also occur in the higher regions of the scatter band and also not all welds with a low A-value are interface failures. Interface failures not only occur beneath some threshold A-value, they occur in the whole scatter range. Interface failures and "good" welds occur side by side on the welded strips.

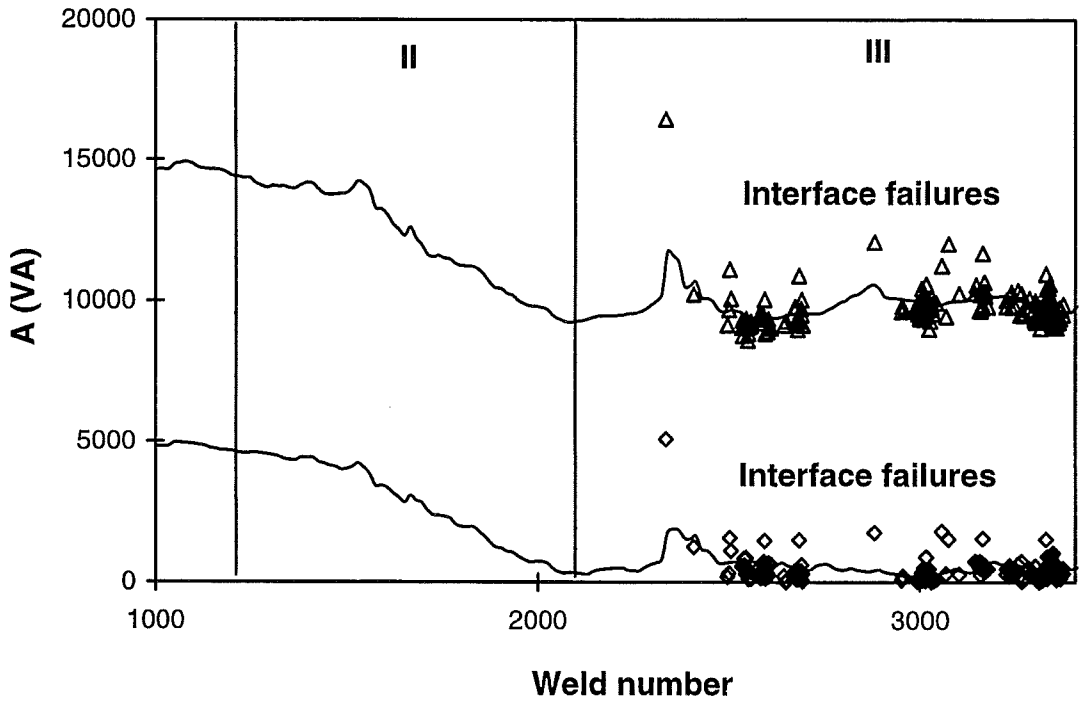

Figure 4.8: Occurrence of interface failures, A-values of interface failures (S1).

The percentage of interface failures in a strip of 45 welds is plotted in figure 4.9. In region-III the strips started to show interface failures at about 2300 welds. The percentage of interface failures strongly fluctuates from almost no interface failure to almost no good weld in a strip, when averaged over a larger sample the percentage of interface failures turns out to be about 30%. It seems that interface failures occur randomly in region III. In this region there is a certain chance a weld turns out to be a interface failure weld, in this case the chance is about 30%. An important observation is that the interface failure welds were only found in region-III. In region-II al strips were free of interface failures. Although not al welds were examined (the first 1000 welds were not tested) it can safely be stated that in region I and II al welds are 100% interface failure free.

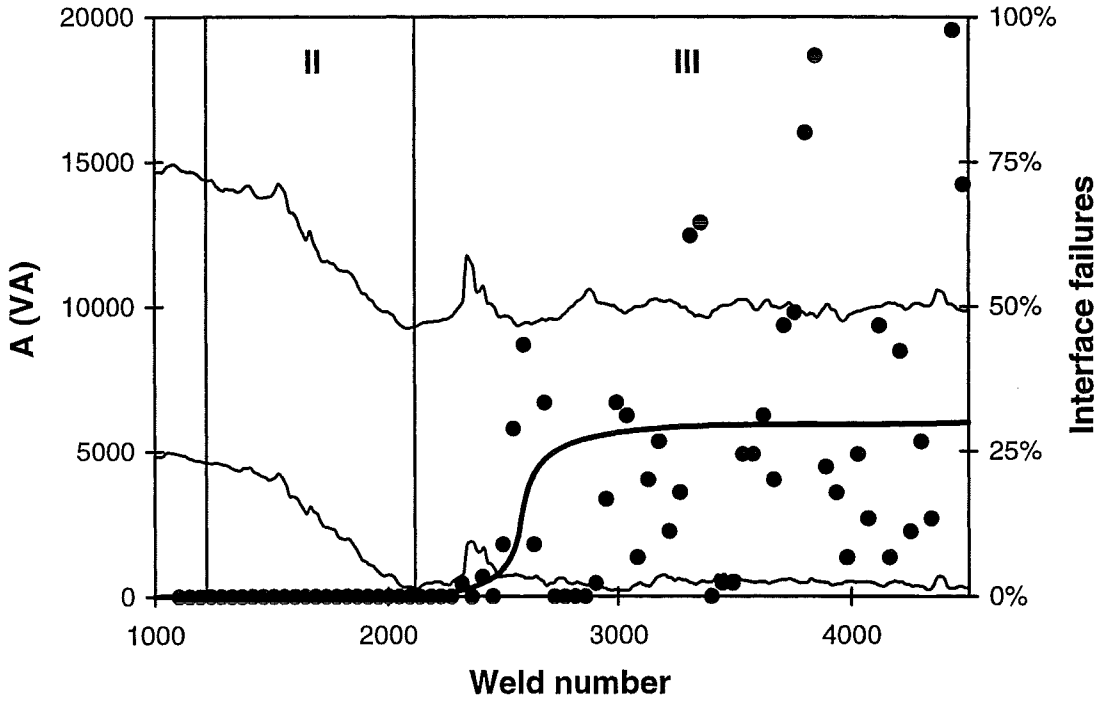

Figure 4.9: Occurrence of interface failures, percentage interface failures (dots and thick line) in strips with 45 welds (S1).

4.3. The 5.5 mm welds

The same settings as for the S1 experiment were used for S2 and S3 welding tests. The results of these three series of welding tests are plotted in figure 4.10. The curves of the S1 and S3 experiments are very similar. Both trials have their first interface failure after approximately 2300 welds. The S2 curves are somewhat different, the curves diminish earlier and slower, region II starts earlier and lasts longer. These differences are contributed to a diminishing welding force, at the start of the experiment. The force was set at 1.8 kN, but during the experiment the force decreased to 1.4 kN. This decrease in welding force was caused by a defect in the pressure regulator. Precautions were taken to prevent the reoccurring of this defect.

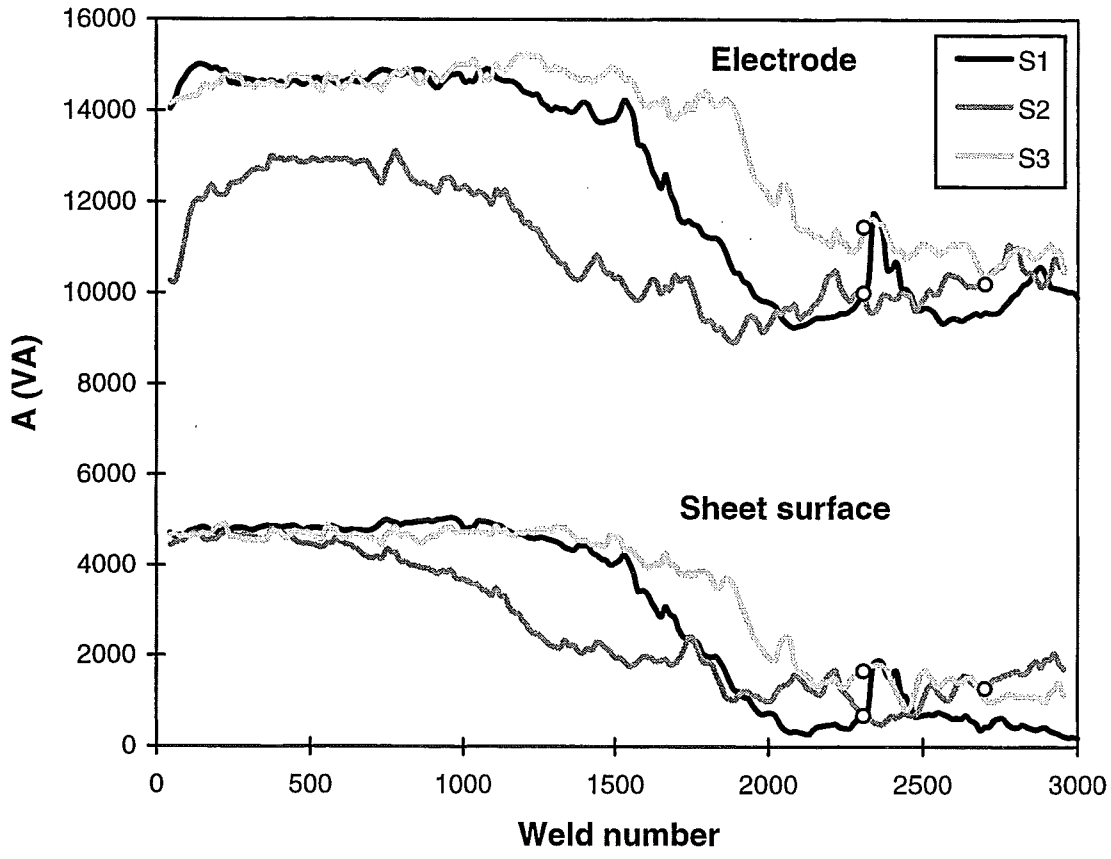

Figure 4.10: Moving average of the loop area values (electrode and sheet surface) for all welding trials with a weld button diameter of 5.5 mm, the markers indicate the first interface failure.

Table 4: Main output of data analysis program for a typical 5.5 mm region-I weld, reprint of table 3 (S1, weld 500).

Half Cycle	t_{aan} (ms)	I_{RMS} (kA)	$V_{sh\text{-}rms}$ (V)	$V_{el\text{-}rms}$ (V)	Q_{sh} (J)	Q_{el} (J)	A_{sh} (VA)	A_{el} (VA)
1	8.7	17.8	204	760	33	126	4646	14335
2	9.4	21.4	128	584	27	125	735	1225
3	9.3	21.3	105	514	22	110	401	571
4	9.4	21.6	93	481	20	104	379	646
5	9.4	21.4	85	460	18	99	106	463
6	9.4	21.7	80	453	17	99	42	388
7	9.4	21.4	77	452	16	97	64	387
8	9.4	21.7	74	455	16	99	89	332

Table 5: Main output of data analysis program for a typical 5.5 mm region-III weld (S1, weld 3000).

Half Cycle	t_{aan} (ms)	I_{RMS} (kA)	$V_{sh\text{-}rms}$ (V)	$V_{el\text{-}rms}$ (V)	Q_{sh} (J)	Q_{el} (J)	A_{sh} (VA)	A_{el} (VA)
1	8.8	18.5	95	614	17	109	72	9466
2	9.4	21.3	132	601	28	128	119	1886
3	9.4	21.2	109	534	23	113	613	1388
4	9.4	21.6	85	477	18	103	258	511
5	9.4	21.4	75	458	16	98	110	379
6	9.4	21.7	71	448	15	97	62	287
7	9.4	21.4	69	445	15	95	59	307
8	9.4	21.7	68	445	15	97	65	228

Samples of the welds made in the S1 and S3 welding trials were used to measure the indentation of the sheet surface by the electrodes, the results are plotted in figure 4.11. New electrodes have a rounded face, the impression therefore is also rounded and relatively deep. During welding the electrodes erode and become flat, the indentation thus also flattens and becomes less deep. The sheet indentation of welds made with new electrodes is about 8% of the plate thickness. Worn electrodes hardly create an impression, the indentation is virtually zero. In figure 4.11 it can be seen that the sheet surface indentation gradual decreases from 8% at the start of the welding trial to zero indentation in region-III.

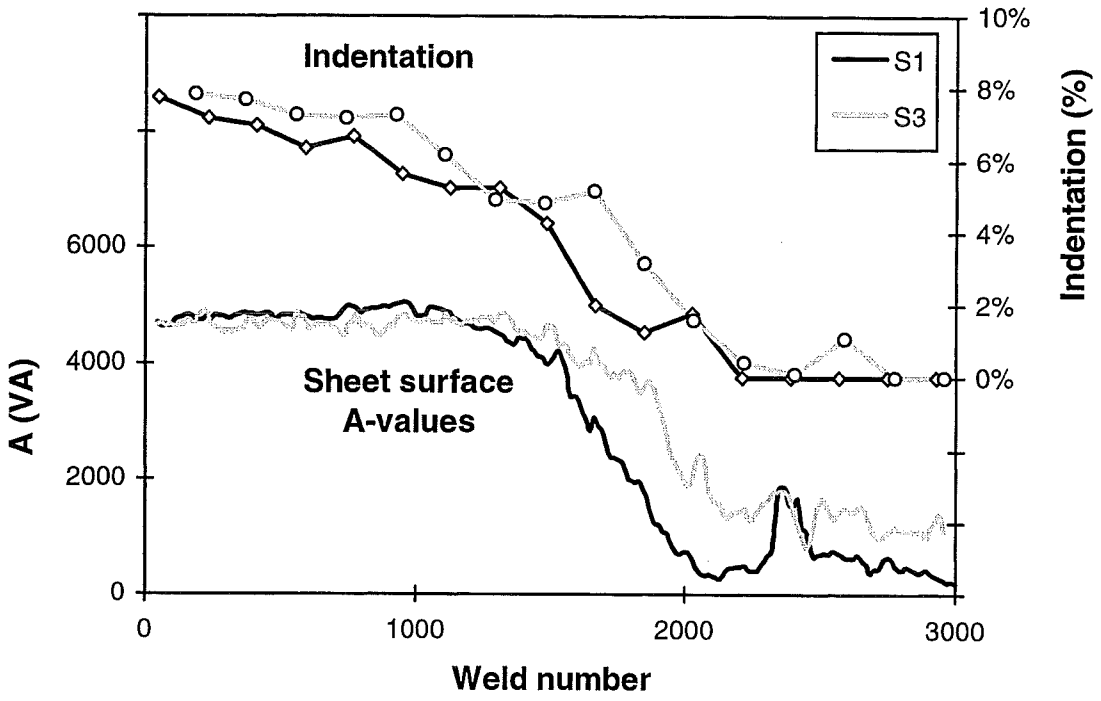

Figure 4.11: Sheet surface indentation sheet surface A-values vs. the number of welds made.

4.4. The 7.0 mm welds

Three welding trials were carried out with the settings for 7.0 mm welds (L1, L2 and L3). The A-curves resulting from these tests are plotted in figure 4.12. The curves show some resemblance with the curves of the 5.5 mm welds, but there are considerable differences between these tests. In the welding tests with 7.0 mm welds the electrodes life was considerably shorter than in the 5.5 mm welding tests. The A-curves do not start with a constant region-I but immediately start to diminish. The electrodes also had a greater tendency to stick to the material. This can be an explanation why the curves are so different from the 5.5 mm curves.

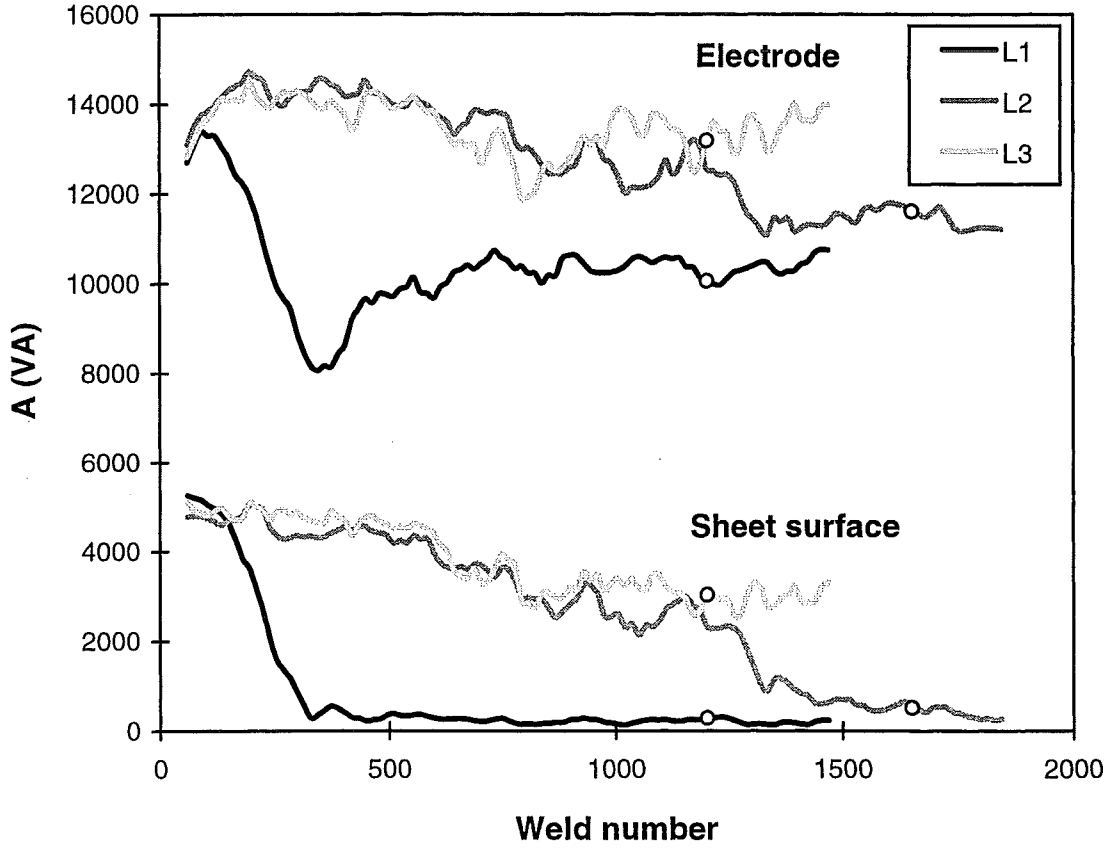

Figure 4.12: Moving average of the loop area values for all welding trials with a weld button diameter of 7.0 mm, the markers indicate the first interface failure.

Table 6: Main output of data analysis program for a typical 7.0 mm region-I weld (L2, weld 250).

half cycle	t_{aan} (ms)	I_{RMS} (kA)	$V_{sh\text{-}rms}$ (V)	$V_{el\text{-}rms}$ (V)	Q_{sh} (J)	Q_{el} (J)	A_{sh} (VA)	A_{el} (VA)
1	8.7	20.6	196	758	37	147	4562	14636
2	9.6	25.3	128	610	32	154	995	1610
3	9.7	25.1	98	536	25	135	305	52
4	9.7	25.5	88	492	22	125	205	107
5	9.7	25.3	79	467	20	118	174	47
6	9.7	25.6	70	447	18	114	100	517
7	9.7	25.3	68	437	17	110	110	83
8	9.7	25.6	69	440	18	112	78	273

Table 7: Main output of data analysis program for a typical 7.0 mm region-III weld (L2, weld 1800).

half cycle	t_{aan} (ms)	I_{RMS} (kA)	$V_{sh\text{-}rms}$ (V)	$V_{el\text{-}rms}$ (V)	Q_{sh} (J)	Q_{el} (J)	A_{sh} (VA)	A_{el} (VA)
1	8.7	20.9	149	660	31	132	430	11533
2	9.6	25.1	167	639	41	160	2095	4088
3	9.7	25.2	114	517	29	130	389	793
4	9.7	25.5	102	492	26	125	278	346
5	9.7	25.3	94	484	24	123	254	375
6	9.7	25.5	88	475	22	121	275	434
7	9.7	25.2	82	467	21	118	108	430
8	9.7	25.6	82	464	21	119	102	379

5. Discussion

5.1. Electrode life & Quality control

An overview of the six electrode life tests is given in table 8. Although the larger 7.0 mm welds have a higher cross tension strength, the strength is increased 25% over that of a 5.5 mm weld, the electrode life is dramatically reduced to about 50% of the electrode life for 5.5 mm welds.

Table 8: Results of the electrode life tests.

	S1	S2	S3	L1	L2	L3
Button diameter (mm) :		5.5			7.0	
Welding current (kA) :		21			25	
Cross tension strength (kN) :		2.4			3.0	
Welds made :	4500	3000	3000	1500	1850	1500
Electrode life :	2300	2700	2300	1200	1650	1200

In the welding tests with weld button diameters of 5.5 mm interface failure welds only occurred in region-III, in this region the A-value (also weld energy Q and welding voltage V_{RMS}) of the welds is low. Also in the welding tests with 7.0 mm welds interface failures started to occur in the lower regions of the A-values. This drop in A-values can be the basis for an on-line quality monitoring system.

Such a system needs a mathematical rule to distinguish between good and bad welds, the most easy rule is a threshold, for instance a threshold sheet surface A-value of half the initial value. For these welding trials this implicates a threshold sheet surface A-value of 2400 VA. The quality control system can then monitor the sheet surface A-values and when the moving average of these values is decreased to a value beneath this threshold value the welding process can be stopped to change the welding electrodes.

Using the threshold of 2400 VA on the sheet surface A-value assures 100% error free welds when welding 5.5 mm welds. The three welding trials all started to show interface failures only after this threshold, even the S2 trial where the welding force was not constant. Two of the three welding trials with 7.0 mm welds comply with this quality control rule, the L3 trial started to show interface failures before the threshold value of 2400 VA was reached.

A quality control rule based on the measurement of the sheet surface voltage needs two additional measuring electrodes alongside the welding electrodes. In an industrial environment this is not very practical. A system based on electrode voltage is more robust (no measuring electrodes which can easily be damaged). The final stationary level of the electrode A-value is

not zero as in the sheet surface A-value. Both the starting level and the final level of the electrode A-value are influenced by distance from the electrode face at which the voltage pickup leads are attached. A quality control rule based on the electrode voltage can for instance be an absolute drop of 2000 VA from the initial A-value. Again all three welding experiments with a weld button diameter 5.5 mm comply with this rule. Also two of the three welding experiments with a weld button diameter of 7.0 mm comply with the rule based on electrode voltage.

Although the cross tension strength of a 5.5 mm weld is 25% below that of a 7.0 mm weld the electrode life is doubled. Also the quality of the 5.5 mm welds is easier to monitor, the 5.5 mm welds can be guarantied 100% error free without the need for destructive tests.

5.2. Dynamic resistance

The dynamic resistance is the momentary resistance when welding, this resistance can be calculated with Ohm's law (V=IR). The resistance at the faying interface (the sheet-sheet interface) can be found with equation 1. If it is assumed that the resistance of the top and bottom electrode-sheet interface are equal then this resistance can be calculated with equation 2.

$$R_{sh-sh}(t) = \frac{V_{sh-sh}(t)}{I(t)} \tag{1}$$

$$R_{el-sh}(t) = \frac{V_{el-el}(t) - V_{sh-sh}(t)}{2 \cdot I(t)} \tag{2}$$

The sheet to sheet resistance is the sum of the resistance of the faying interface and a part of the aluminium sheet resistance itself. The electrode to sheet resistance is the sum of the electrode to sheet interface resistance and a part contributed by the resistance of the aluminium sheet and also a part of the electrode resistance (from the electrode face to the voltage pickup leads). The calculated resistances are the sum of the interface and material resistances.

The dynamic resistance curves for a typical region-I weld are plotted in figure 5.1. The dynamic resistance of the electrode to sheet interface is about twice that of the sheet to sheet interface resistance. The resistance falls a decade in value in less than 5 ms (less than ¼ period). This is caused by the rapid growth of the conducting a-spots. After this initial fall the dynamic resistance still decreases but only slightly.

For a typical region-III weld the dynamic resistance curves are shown in figure 5.2. Although the welding electrodes are worn, the electrode face has become flat and rough, the electrode to sheet dynamic resistance curve remains the same. Both the level as well as the form of the dynamic resistance curve for the electrode to sheet interface are unaffected by the deterioration of the welding electrodes.

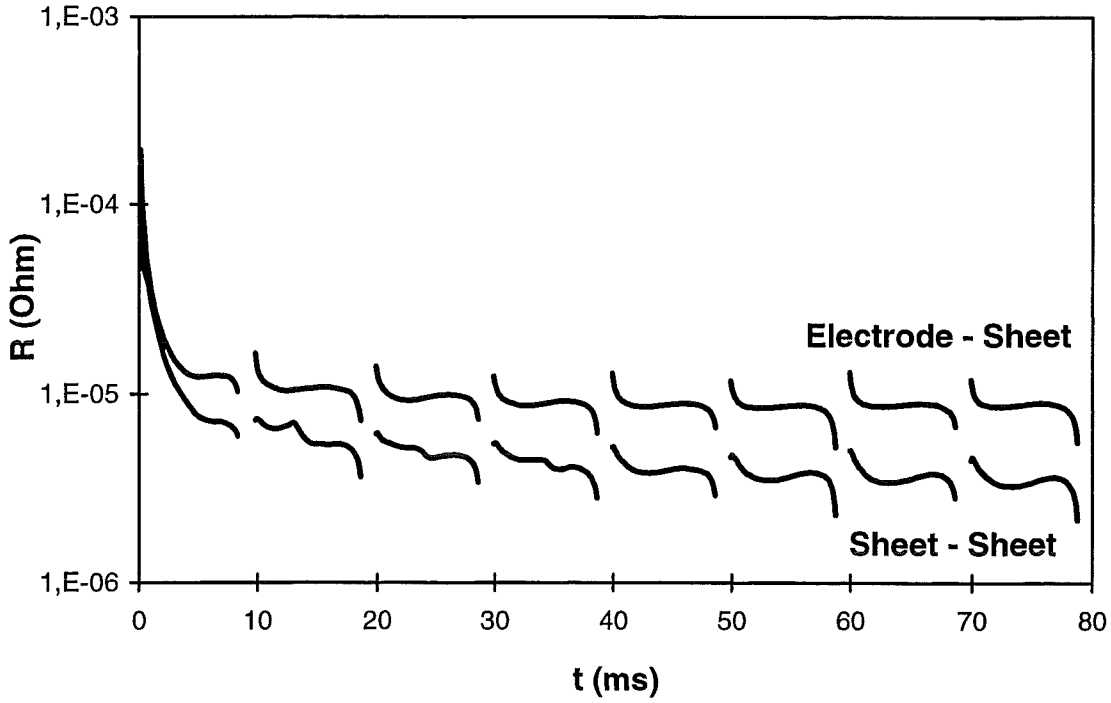

Figure 5.1 Dynamic resistance curves for a typical region-I weld (S1, weld 500).

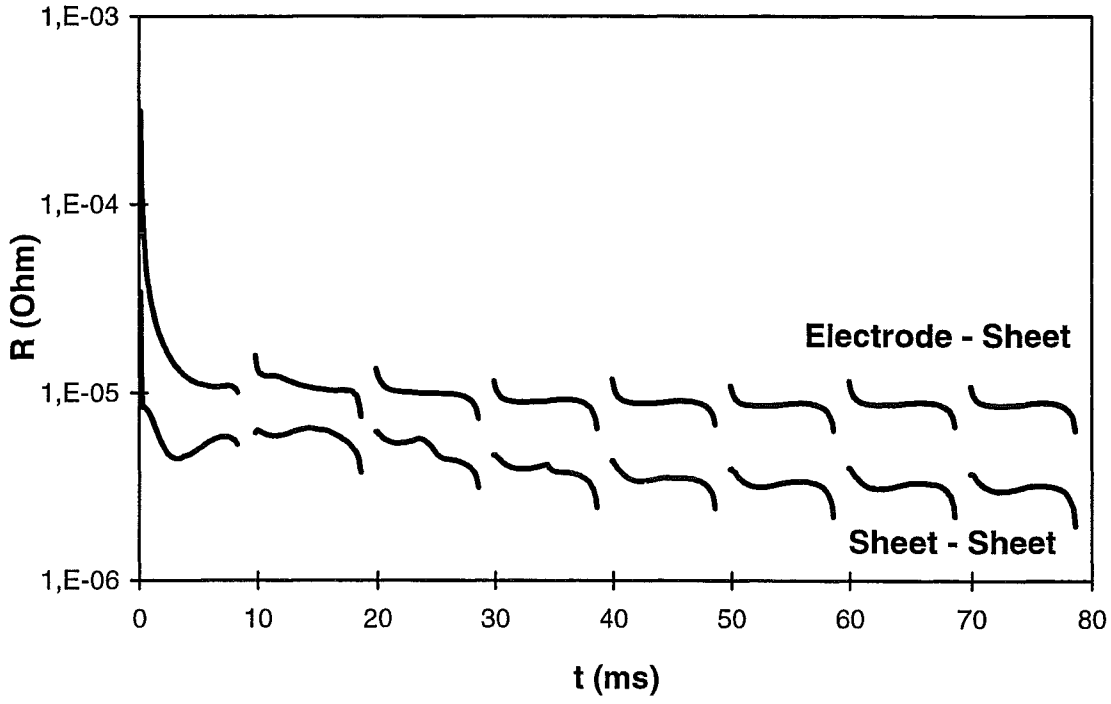

Figure 5.2: Dynamic resistance curves for a typical region-III weld (S1, weld 3000).

At the sheet to sheet interface the situation is different, the sheet surfaces are still the same (always fresh surfaces) but the dynamic resistance curve has changed. The initial sheet surface resistance of the region-III weld is much lower than for the region-I weld, although the surface state of the aluminium is still the same. An altered situation at the electrode-sheet contact (the electrode face has become flat and rough) causes a change in dynamic resistance at the faying interface.

The altering dynamic resistance curve of the sheet-sheet interface is the cause of the diminishing of the loop area for the first half cycle of welding and thus also for the decreasing values for the welding voltage (V_{RMS}) and welding energy (Q) in the first half cycle of welding.

The surprising observation that the dynamic resistance curve of electrode to sheet interface is unaffected by the deterioration of the electrode can also be seen in one of the earlier figures. In the figure in which the voltage for the first half cycle of welding is plotted, the drop in voltage from the level of region-I to the level of region-III has about the same value for both the electrode voltage as for the sheet surface voltage. The drop in voltage measured on the electrode is entirely caused by the drop in sheet surface voltage (faying interface voltage). The electrode to sheet voltage is not affected by the deterioration of the electrodes, only the sheet surface voltage is affected. A satisfactory explanation for this phenomenon has not been found.

The decrease in welding energy affects the geometry of the welds, this can be seen in the figures 5.3 and 5.4. A typical region-I weld is shown in figure 5.3, the impression is rounded as are new welding electrodes. The typical region-III weld in figure 5.4 has no impression, the welding electrodes are flattened by the erosive deterioration. Both welds are about 5.5 mm in diameter (both were welded with a current of 21 kA), also both welds are porous. This porosity can also be seen on X-ray photographs made of weld samples (not included here). Internal defects tend to play a relatively insignificant role in the fracture initiation process, since the critical stress concentration is located on the weld periphery [17].

The difference between the two welds is their size, the width (diameter) is about the same but the height of the region-I weld is much greater. The weld pool of the region-I weld is larger, it has penetrated the aluminium sheet deeper than the region-III weld. The sheet penetration of the region-I weld is about 85% whereas the penetration of the region-III weld is about 65%.

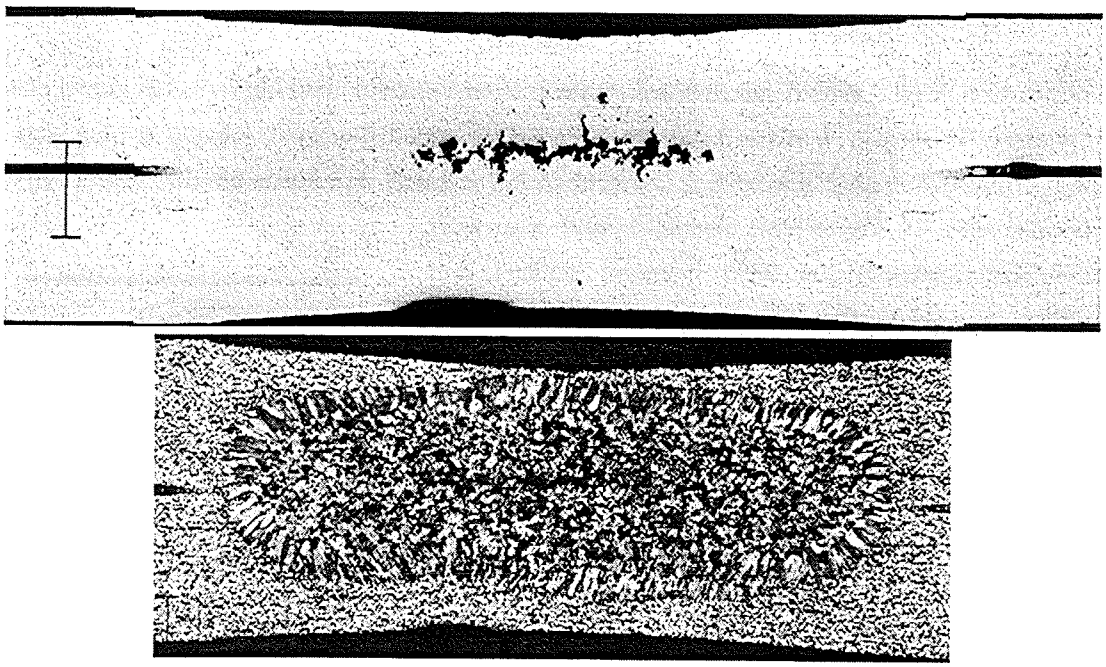

Figure 5.3: Cross section of a typical region-I weld (5.5 mm weld button diameter).

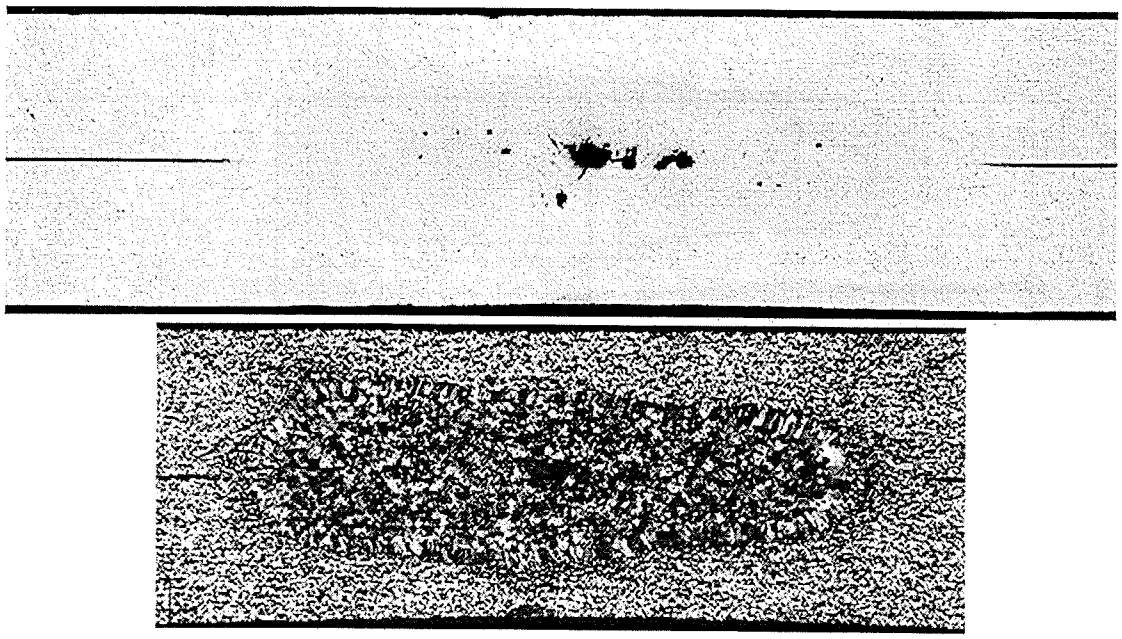

Figure 5.4: Cross section of a typical region-III weld (5.5 mm weld button diameter).

5.3. Plug or interface failure

When spot welded sheets are pulled from each other the welds can basically fail in two different manners or modes. The plate can be sheered off round the weld, leaving a plug and hole (mode-p), in this case the weld is stronger than the sheet. The force needed to pull a plug is proportional to the sheet thickness and the weld diameter, because the weld diameter doesn't drift during a welding trial the mode-p strength is fairly constant. The other mode of failure occurs when a weld fractures along its faying surface (mode-i), this is called an interface failure. The strength of a interface failure is determined by the strength of the weld itself.

Welds that fail as interface failures (mode-i) are considered to be bad welds, they have a low quality. When welds pull a plug they are considered to be good welds, even in region-III. Thus even as the neighbouring welds fail as interface failures the welds that pull a plug are considered to be good welds.

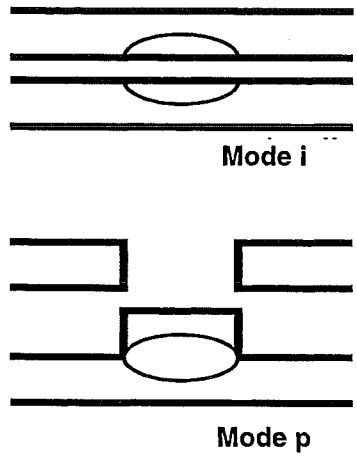

Figure 5.5: Two types of weld failure mode-i (interface failure) and mode-p (plug).

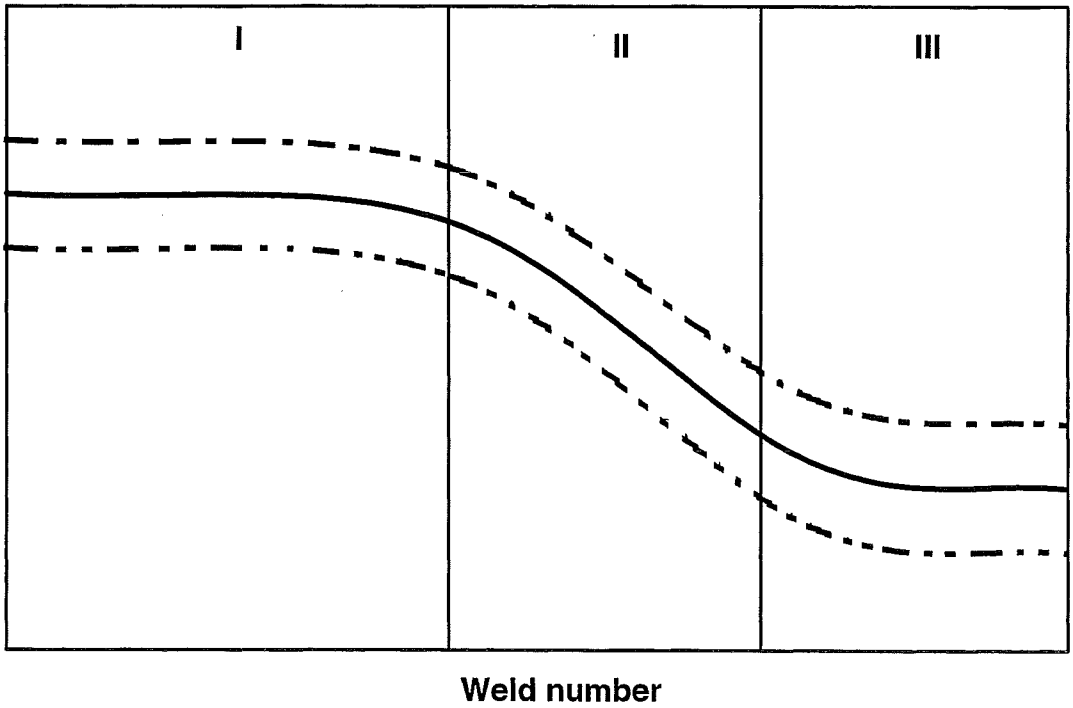

Figure 5.6: Generalised trend seen in different welding parameters.

The trend shown in figure 5.6 is observed for a lot of parameters (V_{RMS}, Q, A), suppose that this trend is also present in the strength of the weld itself. Assume that the strength of the weld itself, the mode-I strength shows the trend depicted in figure 5.6. The cross tension strength of a weld is fairly constant over the electrode life this is caused by the fairly constant diameter of the welds, thus the mode-p strength is constant (with some scatter) over the electrode life. Suppose the weld has a certain strength and a certain scatter in this strength as depicted in figure 5.7. This would explain why in region I and II al welds fail in mode-p (pull a plug) and why in region-III the welds fail both in mode-p as in mode-i.

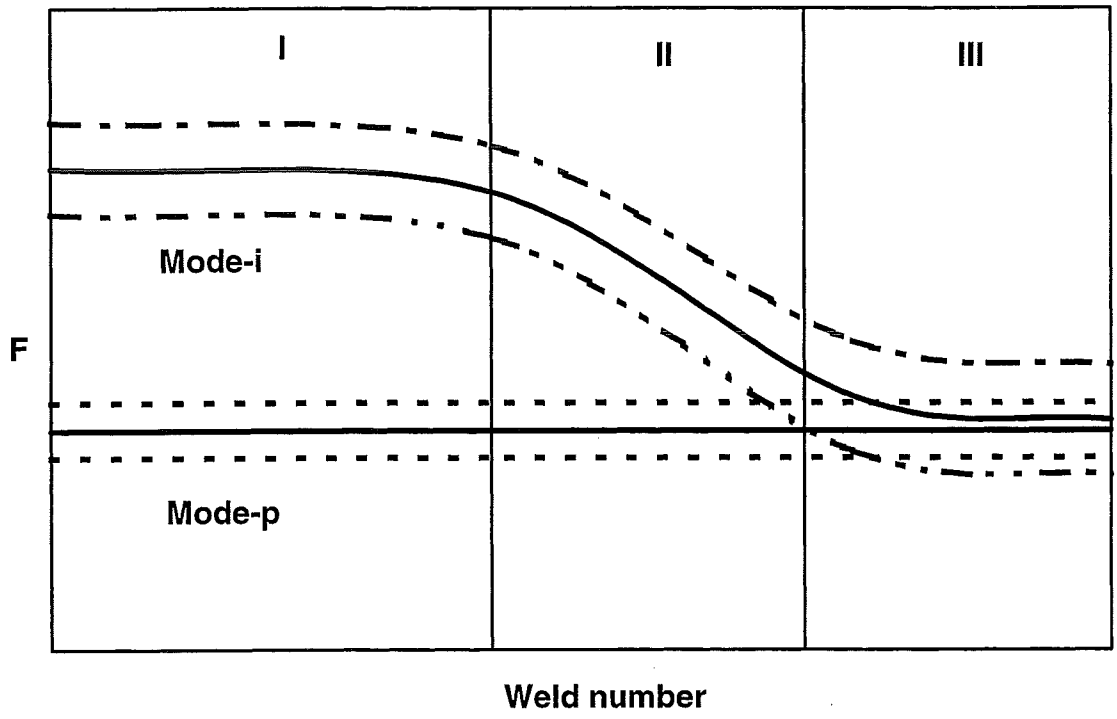

Figure 5.7: Proposed diagram for the strength of the two weld failure modes.

In region-I the strength of the welds is on a high level, the sheer strength of the sheet is far less than the strength of the welds itself. In region-II the weld strength starts to diminish but this strength is still higher than the mode-p strength. Thus in a destructive test the welds still fail in mode-p and pull plugs. When region-III is achieved the mode-i strength is decreased to the level of the mode-p strength and the scatter bands of both modi overlap and the situation becomes critical. This overlap causes the welds to have a certain chance on either failure mode, for instance if the weld strength is on the low side and the sheet strength is rather high the weld will fail as an interface failure.

In this new approach all welds in region-III are considered of low quality and not only those who failed as interface failure in a destructive test. It would be advantageous to measure the weld strength directly. This requires a test method in which the weld can only fail in mode-I (across its interface). Good candidates for such a test method should be sheer tests and torsion tests. Impact tests and other mechanical properties should also be considered when measuring weld quality. Weld quality, as far as strength is concerned, should not only be assessed on basis of a plug or a interface failure in tensile loading tests. For fatigue behaviour a further and in-depth investigation should be carried out.

6. Conclusions

- For the experiments carried out the welding machine can be considered a constant current source. This is caused by a relatively high internal resistance of the welding machine (combined with a constant mains voltage).
- The first half cycle of welding contains the most information about the welding process, it is the most important half cycle during welding. This is because of the sharp decrease in dynamic resistance when spot welding aluminium, within the first half cycle the resistance decreases almost to its final level.
- The welding voltage (V_{RMS}) and the welding energy (Q) curves all show the same trend. For the first welds (region I) the signal is constant, after which it drops over the following welds (region II) after this it again has a more or less constant value (region III).
- Both the level and the form of the dynamic resistance curve for the electrode to sheet interface are unaffected by the deterioration of the welding electrodes. At the sheet to sheet interface the situation is reversed, the sheet surfaces are still the same (always fresh surfaces) but the dynamic resistance curve changes. An altered situation at the electrode-sheet contact (the electrode face has become flat and rough) causes a change in dynamic resistance at the faying interface. A satisfactory explanation for this phenomena has not been found.
- Interface failure welds were only found in region-III. In this region the interface failures seem to occur randomly, in region-III there is a certain change a weld turns out to be an interface failure.
- In region-III the A-value and also the weld energy Q and the welding voltage V_{RMS} of the welds is low. This drop in A-values can be the basis for an on-line quality monitoring system.
- Although the cross tension strength of a 5.5 mm weld is 25% below that of a 7.0 mm weld the electrode life is doubled. Also the quality of the 5.5 mm welds is easier to monitor, the 5.5 mm welds can be guaranteed 100% error free without the need for destructive testing.
- Welds that fail as interface failures are considered to be bad welds, they have a low quality. When welds pull a plug they are considered good welds, even in region-III. Thus even as the neighbouring welds fail as interface failures the welds that pull a plug are considered to be good welds. In the proposed model all welds in region-III are considered of low quality and not only those who fail as interface failure in a destructive test.

- It would be advantageous to measure the weld strength directly, this requires a test method wherein the weld can only fail in mode-I. Good candidates for such a test method should be sheer tests and torsion tests. Impact tests and other mechanical properties (such as fatigue strength) should also be considered when measuring weld quality. Weld quality, as far as strength is concerned, should not only be assessed on basis of a plug or a interface failure in tensile loading tests.

References

[1] G.L. Lazzarani
Weerstandpuntlassen van aluminiumlegeringen
Aluminium, nr.5 1993

[2] G. den Ouden
Lastechnologie
Delftse Uitgevers Maatschappij, Delft, 1993

[3] R. Heimbuch, A. Houchens, J. Thomas
Contact resistance of 2036-T4 aluminium and its effect on resistance spot welding
ASM confr. "Technological impact of surfaces - Relationship to forming welding and painting" , Dearborn Mi, april 1981, 179-206

[4] A.W.M. Bosman
Weerstandslassen van aluminiumlegeringen, de stand van zaken
Lastechniek, mei 1997

[5] E. Østgaard
Spot welding aluminium as delivered
Metal construction, february 1980, 78-86

[6] E.P. Patrick, D.J. Spinella
Surface effects on resistance spot weldability aluminium body sheet
IBEC '95, Body assembly & manufacturing, 1995

[7] D.J. Spinella
Implications for aluminium resistance spot welding using alternating current
IBEC '95, Materials & body testing, 1995

[8] J.R. Auhl, E.P. Patrick
A fresh look at resistance spot welding of aluminium automotive components
SAE int. congr. & exposition, Detroit MI, march 1994

[9] E.P. Patrick, J.R. Auhl, T.S. Sun
Understanding the process mechanisms is key to reliable resistance spot welding aluminium auto body components
SAE Technical Paper 840291, 1984

[10] R. Holm
Electric contacts Handbook
Springer-Verlag, Berlin, 1958

[11] J.A. Greenwood
Constriction resistance and the real area of contact
British journal of applied physics, vol. 17 (1966), 1621-1632

[12] P.H. Thornton, A.R. Krause, R.G. Davies
Contact resistances in spot welding
Welding journal research supplement, december 1996, 402s-412s

[13] F.R. Hoch
Joining of aluminium alloys 6009/6010
SAE congr. and exposition, Detroit Mi, march 1978

[14] F. Arthur, S. Handley, K. Osman, C. Wallet
Welding of aluminium in the automotive industry
Autotech '89, Int. bus, truck and car product and manufact. (1989)

[15] W.L. Roberts
Resistance variations during spot welding
The welding journal, november 1951, 1004-1019

[16] O.J. Hana
Review of the spot welding of aluminium
Internal rapport Hoogovens

[17] P.H. Thornton, A.R. Krause, R.G. Davies
The aluminium spot weld
Welding journal research supplement, march 1996, 101s-108s

Appendix

A.1. Data analysis program

The welding trials generated a lot of data. A weld data analysis program was used to cope with these massive data sets. The program code was developed by the author specially for this research project. The data analysis program can extract a number of parameters from the stored current and voltage waveforms The program consists of the following basic steps:

- Read data: The current, electrode and sheet surface voltage waveforms as well as the signal from the compensation coil are read from disk and stored in memory for further processing.
- Find current wave tops: The maxima in the absolute value of the current signal are found for each half cycle, this results in 8 current wave tops.
- Find on-off: The start and end time of each halfcycle is determined. When the current is shut on or off the second derivative of the current has sharp peaks, this is used to determine the start and end of the halfcycles.
- Compensation: The compensation for the inductive component in the measured voltage signals is done by subtracting the scaled signal from the compensation coil from the measured voltage signals. A constant resistance is resembled by a strait line in a VI-diagram, this is used to determine the scaling factor. In the last half cycle of welding the dynamic resistance is fairly constant, the loop in the VI-diagram for this half cycle therefore should be a straight line and have no area. Having determined the scaling constants for the compensation the voltage signals can be corrected.
- Determine A-values: Now the start and end of each half cycle is known and the voltage signals are cleaned from their inductive components, other parameters can be calculated. The values for the loop areas (A-values) are found by integrating Vdl over each half cycle.
- Determine other values: The other parameters can now also easily be calculated. True RMS. (root mean squired) values are calculated for each half cycle of current, sheet surface and electrode voltage. The generated energy is calculated by integrating (V•I)dt over each half cycle. Voltage wave tops are also determined again for each half cycle.
- Output: Al these parameters are stored on disk.

These steps are repeated until the data of all welds is processed.

A.2. Modelling the current

A spot welding machine consist of a few basic elements, there is a transformer, a thyrystor (for heat control) and there is the throat of the machine. The transformer is a kind of AC power source, the thyristor is a special sort of switch and the throat is a sort of coil thus an inductance and all these parts have a resistance.

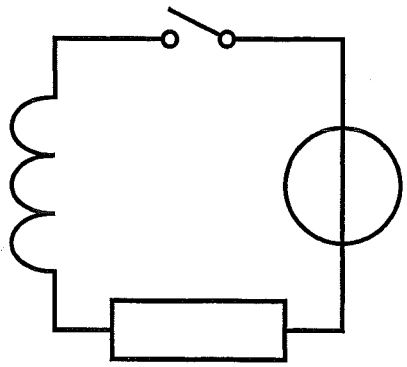

Figure A2.1: Simplified welding circuit.

A circuit of the kind shown in figure A2.1 should be able to model the welding current, this circuit consists of:

power source : $V_{source} = E_0 \sin(\omega t)$

resistance : $V_R = R\,I$

inductance : $V_L = L\,dI/dt$

In these equations ω is the angular velocity of the alternating power source ($\omega=100\pi$ rad/s) this is equivalent with the frequency of the source (f=50 Hz). When the switch is open there can not flow a current through the circuit but when the switch is closed then the following equation is true:

$$V_{source} = V_R + V_L \tag{A2.1}$$

this leads to the differential equations A2.2.

$$E_0 \sin(\omega t) = RI + L\frac{dI}{dt} \tag{A2.2}$$

Rewriting this equation leads to the following differential equation (with starting value):

$$\frac{dI}{dt} = \frac{E_0}{L}\sin(\omega t) - \frac{R}{L}I(t), \quad I(t_{start}) = 0 \tag{A2.3}$$

As can be seen the problem is not described by four parameters (E_0, R, L and t_{start}) but with one less. The problem can be described with three parameters (here E_0/L, R/L and t_{start}). The parameters E_0, R and L are characteristics of the welding machine, t_{start} is set by the heat control unit.

The differential equation A2.3 can be solved, the following equation is a solution of the differential equation.

$$I(t) = f(t) - e^{-\frac{R}{L}(t-t_{aan})} \cdot f(t_{start})$$
$$f(t) = \frac{E_0 L}{R^2 + \omega^2 L^2}\left(\frac{R}{L}\sin(\omega t) - \omega\cos(\omega t)\right) \qquad \text{(A2.4)}$$

This solution consists of a long and short term part. The long term part is the f(t) part, the rest is the short term part. The short time is an exponential function which decays rapidly in time, the function of this part of the equation is to satisfy the starting condition. The longer term is the solution of the problem for larger times, this long term predominates the solution after the first cycle.

Heat control opens the circuit when the current is zero again (after the first half cycle) and re closes the circuit after a little while. For the current waveform when welding with heat control only the first half cycle of the solution is of importance. The heat control can adjust the current waveform by adjusting the ignition point (t_{strart}) for each half cycle.

The dynamic welding machine parameters can be extracted from the current waveforms, R/E_0 and L/E_0 were extracted. The open voltage of the welding machine (V_{open}) is determined by the transformer tap setting. For both used transformer tap settings this open voltage was measured (see table). The open voltage is an RMS. voltage, E_0 is the amplitude of this voltage and can now be calculated ($E_0=V_{open} \bullet \sqrt{2}$).

Transformer tap :	23	24
V_{open} (V) :	7.33	8.69
E_0 (V) :	10.4	12.3

The dynamic parameters of the welding machine (R and L) can now also be calculated.

$$R = 1.86 \bullet 10^{-4}\ \Omega\ (^{V}/_{A})$$
$$L = 8.34 \bullet 10^{-7}\ H\ (^{Vs}/_{A})$$

In this calculation it is assumed that the resistance (R) is constant but the resistance of the aluminium during welding is dynamic in nature. This is not a problem because the internal resistance of the machine is greater than the resistance of the aluminium, the fall in dynamic resistance during welding has only a small effect on the total resistance. The relatively high internal resistance prohibits the current to be affected by a change in the external resistance. The inductance (L) may also be considered a constant and because the mains power voltage was relatively constant E_0 may also be considered constant. Thus a relatively high internal resistance (combined with a constant mains voltage) causes the welding machine to behave as a constant current source.